ACCEPTED MANUSCRIPT

Influence of TiO2 and MWCNT nanoparticles dispersion on microstructure and mechanical properties of Al6061 matrix hybrid nanocomposites

Influence of TiO₂ and MWCNT Nanoparticles Dispersion on Microstructure and Mechanical Properties of Al6061 Matrix Hybrid Nanocomposites

Sourabh Kumar Soni[1] and Benedict Thomas[2]*

[1, 2*] *School of Mechanical Engineering, Vellore Institute of Technology, Vellore, 632014, Tamil Nadu, India.*
Corresponding author. E-mail: benedict.thomas@vit.ac.in

Abstract

The influence of nanoparticle agglomeration plays a crucial role in altering the mechanical properties of the resulting nanocomposites. The pre-processing of nanoparticles prior to its addition in the matrix alleviates the agglomeration and helps to attain the uniform dispersion. In the present work, an ultrasonic-assisted stir/squeeze casting technique was employed to prepare the aluminum 6061 (Al6061) based hybrid nanocomposites reinforced with pre-processed TiO₂ and multi-walled carbon nanotubes (MWCNTs). In order to achieve uniform dispersion of nano-reinforcements on resulting Al-based hybrid nanocomposites, four different reinforcements pre-processing routes, i.e. sonication, ball-milling, stirring and its combinations were adopted. The effects of numerous parameters such as reinforcement weight percentage, reinforcement pre-processing routes and fabrication techniques on the microstructure and mechanical properties of the hybrid nanocomposites were investigated. The effect of various pre-processing routes on the morphology evolution in MWCNTs and TiO₂/MWCNT nanoparticles mixture were investigated using scanning electron microscopy (SEM), transmission electron microscopy (TEM) and X-ray diffraction (XRD) techniques. Further, the microstructural investigation of the prepared nanocomposites was carried out by employing optical microscopy (OM) and x-ray mapping analysis. Mechanical characterizations such as tensile strength and microhardness show significant enhancement in the mechanical properties of hybrid nanocomposites due to the addition of pre-processed nano-reinforcements. The

ultimate tensile strength (UTS), yield strength (YS) and microhardness of the ultrasonic-assisted squeeze cast Al6061-TiO$_2$ (1 wt%)-MWCNT (1.5 wt%) hybrid nanocomposite remarkably enhanced by 302%, 400% and 77 %, respectively, due to MWCNTs shortening, uniform dispersion of reinforcements and processing technique. The fractured surface morphology of hybrid nanocomposites was examined using Field Emission-SEM, which exhibits the presence of nano-reinforcements without any sign of destruction in their morphology.

Keywords: Multi-walled carbon nanotubes; Aluminium-based hybrid metal matrix nanocomposite: Microstructure investigation; Dispersion; Ultrasonic-assisted Casting: Mechanical properties.

1. Introduction

The multi-walled carbon nanotubes (MWCNTs) are first synthesized by Iijima et al. [1] in 1991 through the arc discharge technique. Significant efforts are made by several researchers to employ this ultimate nanofiller in polymers, metals and ceramic matrix to develop novel nanocomposites. This nanomaterial is recognized as an ultimate nanofiller due to its exceptional mechanical properties, i.e. high modulus up to 4.15 TPa [2] and tensile strength up to 150 GPa [3], which is helpful to strengthen the resulting nanocomposites, unlike conventional fillers. Numerous research work has been carried out in the fabrication and characterization of carbon nanotubes (CNTs) reinforced polymer and fiber-matrix composites in the last few decades. Whereas, presently, researchers are giving significant attention to the development of CNT-reinforced metal matrix composites (MMCs) due to its promising applications towards automobile, marine and aerospace industries [4–7].

In the arena of advanced lightweight high-strength MMCs, aluminum alloys are the most popular owing to its decent mechanical properties and low density as compared to other matrix

materials. Literature shows that aluminum metal matrix composites (AMMCs) are widely accepted in the field of automobile, marine, sports goods industries and aircraft components due to its excellent corrosion resistance, mechanical, physical, tribological, electrical and thermal characteristics [8,9]. In the recent era, AMMCs reinforced with CNTs gain stimulated research attention and become a topic of prevalent research work among the researchers due to its excellent mechanical, thermal, physical and corrosion resistance characteristics. Owing to that, this newly developed aluminum metal matrix nanocomposites (AMMNCs) found its application towards aerospace and automotive components [10]. AMMNCs can be fabricated through various fabrication techniques such as friction stir processing [11,12], powder metallurgy [13,14], stir casting [15] and squeeze casting [16]. A significant number of research articles on fabrication, microstructural examination, strengthening mechanism and mechanical characterization of the AMMNCs have been observed, which demonstrates substantial improvement in the properties of the AMMNCs.

Attaining uniform dispersion and engagement of distinct CNTs in the matrix without damaging its tubular structure and morphology are major challenges during the fabrication of AMMNCs. These problems are mainly due to the CNT agglomeration caused by van der Waals interactions and its high aspect ratio. To overcome these problems, various dispersion techniques such as sonication, stirring, ball-milling (low and high energy), magnetic stirring and nanoscale dispersion technique were reported by several researchers [5]. The combination of the above-discussed techniques is also used by earlier researchers to obtain uniform dispersion. It is observed from the literature that the combination must be perfect in order to avoid any damage or destruction of the CNT tubular structure. Moreover, various studies revealed that the nanotubes morphology and their dispersion techniques/time also play a significant role in altering the mechanical properties of the AMMNCs. Outcomes presented by Simões et al. [17] demonstrated that the nanotubes morphology and its dispersion significantly affect the

mechanical properties (UTS and microhardness) of the resulting nanocomposites. Therefore, investigations on the effects of several dispersion techniques such as sonication and ball-milling on MWCNTs dispersion and morphology require critical attention and still have immense scope for further investigation.

On the other hand, due to growing demands of new materials with improved service life, reduced weight and economical features, several studies are being carried out to enhance the mechanical properties of the AMMNCs by reinforcing micro and nano-ceramic particles such as Al_2O_3 [12], B_4C [18], Graphene/Al_2O_3 [19] and SiC [20]. Ceramic nanoparticles in aluminum alloy demonstrated good wettability in melt and superior mechanical properties compared to other reinforcements [21]. Further, literature divulged that the employment of hybrid reinforcement in Al-based hybrid nanocomposite is better than single reinforcements [22]. So far, trivial investigations have been performed on the fabrication and characterization of aluminum metal matrix hybrid nanocomposites (AMMHNCs), and efforts are made to examine its effect on the augmentation of mechanical properties of resulting nanocomposites. Also, the influence of reinforcement dispersion on the strengthening of hybrid nanocomposites are unexplored and need critical investigation.

Among all the AMMCs fabrication techniques, stir/squeeze casting (liquid-state processing) is observed to be a better preparation method due to its simplicity in operation, inexpensive, continuous matrix media and higher production rate [23]. However, agglomeration of nanomaterials, poor wettability of reinforcements and non-homogenous mixing (clustering) of nano-reinforcements in stir casting restricts feasible attainment of preferred mechanical properties of AMMHNCs [24]. Some researchers have adopted the ultrasonic-assisted casting techniques to reduce the chances of nanomaterial agglomeration and non-homogenous mixing of nano-reinforcements in the matrix. Nevertheless, owing to high melt viscosity still, some agglomeration and clusters were observed in the prepared composites [25]. The existence of

such agglomeration and non-uniform mixing of nano-reinforcements in the prepared specimens reduces the strength, ductility and stiffness of the resulting hybrid nanocomposites. Pre-processing (pre-dispersion) of nanomaterial/nano-reinforcements, prior to its addition in the melt might be a better approach to reduce the chances of nanomaterial agglomeration and non-uniform mixing of nano-reinforcements. Therefore, further investigation in the pre-processing of nanomaterial/nano-reinforcements by using various dispersion techniques is needed [4]. Also, it can be believed that the ultrasonic-assisted stir casting approach can be a better fabrication route if the difficulties associated with the dispersion uniformity of nanomaterial and uniform mixing of nano-reinforcements in the matrix is eliminated.

Al6061 alloy is widely accepted for structural applications such as pipelines, railroad cars, automobile and marine frames due to higher toughness, decent corrosion resistance, reasonable strength as well as easy to work, weld and machine [9]. Further, commercial and technical utilization of these alloys can be enhanced by improving their mechanical characteristics. So far, very few studies on the employment of hybrid reinforcement, including SiC/Graphite [24,26], Al_2O_3/h-BN [27,28], Al_2O_3/TiB_2 [29] and Graphene/h-BN [22] on Al-based composites by using ultrasonic-assisted stir/squeeze casting technique are reported. Also, studies on the Al6061-MWCNT-TiO_2 hybrid nanocomposites are seldom found.

TiO_2 nanoparticles are promising reinforcement for numerous AMMCs owing to its strong bonding with matrix material as well as exceptional physical and mechanical characteristics. It is also believed that the wettability of these nanoparticles with aluminum was adequate for the fabrication of AMMHNCs with high strength performance [21,30]. Moreover, according to literature, reinforcement of 1.5 wt% of MWCNTs was found to be appropriate content and demonstrates substantial improvement in the mechanical properties of resulting nanocomposites [31–33]. Also, it can be perceived that the reinforcement of nano-size ceramic and nanomaterial mixture in Al6061 alloy can improve its applicability for aircraft applications

and automobile industries such as cylinder liners, engine components, brake shoes and landing gears. Hence, it is necessary to examine the role of TiO_2 and MWCNT nanoparticles on the strengthening of hybrid nanocomposites along with microstructure analysis.

The present work deals with the fabrication of Al6061-TiO_2-MWCNT nanocomposites reinforced with pre-processed TiO_2/MWCNT nanoparticles through ultrasonic-assisted stir and squeeze casting. Prior to the fabrication, the effect of sonication and ball-milling time on dispersion uniformity and microstructure of MWCNTs were examined by SEM and TEM. Further, microstructure analysis of TiO_2/MWCNT nanoparticles mixture dispersed by different pre-processing routes and mechanical characterization of Al6061-TiO_2 (1 wt%)-MWCNT (0, 0.5, 1 and 1.5 wt%) nanocomposites have also been performed to investigate the effect of ceramic and nanomaterial reinforcement as well as the effectiveness of different reinforcement pre-processing routes.

2. Materials and methods

In this work, MWCNTs and TiO_2 nanoparticles were used as the reinforcing phases and Al6061 alloy as the matrix phase for the fabrication of the AMMHNCs. MWCNTs (purity > 99%, diameters 5–40 nm and lengths 1–5 µm) were procured from Ad-Nano Technologies Private Limited, India. TiO_2 nanoparticles (particle size 50–200 nm) were obtained from Nano Research Lab, India. The details of the chemical composition of Al6061 alloy are given in **Table 1**. The morphology of the as-received MWCNTs and TiO_2 nanoparticles are presented in **Fig. 1.**

Table 1
Chemical composition of Al6061 alloy (in wt%).

| Mg	Si	Mn	Cu	Fe	Ti	Zn	Cr	Al
0.88	0.70	0.33	0.29	0.18	0.02	0.003	0.006	97.591
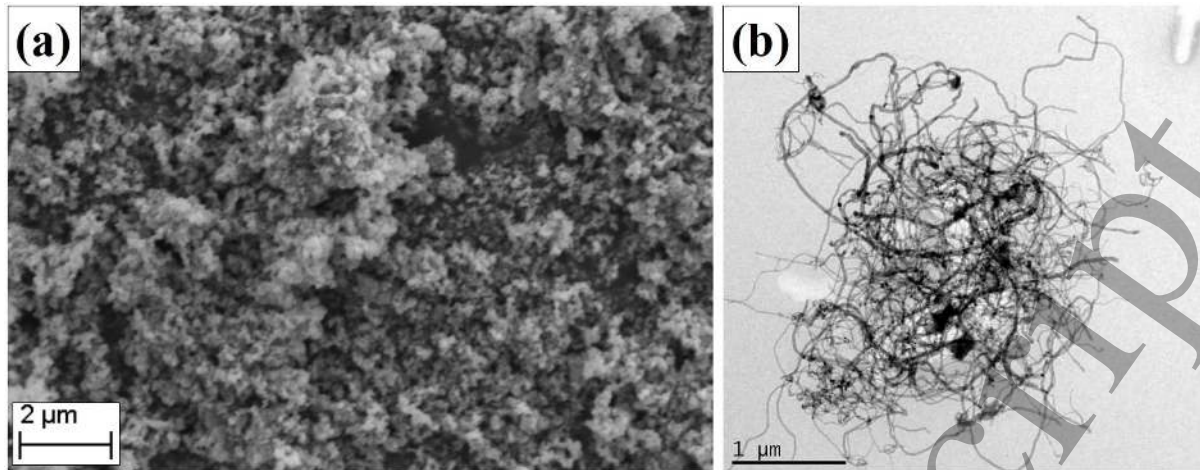
Fig. 1. (a) SEM image of TiO$_2$ nanoparticles and (b) TEM images of MWCNTs.

2.1 Fabrication of Al6061-TiO$_2$-MWCNT nanocomposites

It has been already discussed that the mechanical stirrer and ultrasonic probe used in ultrasonic-assisted stir/squeeze casting are not much effective approach to attain the uniform dispersion of nano-reinforcements in the matrix. Hence, in the present work, prior to the fabrication of nanocomposites, different reinforcement pre-processing (dispersion) routes have been adopted to achieve uniform mixing, improved wettability and homogenous dispersion of nano-size TiO$_2$ and MWCNTs (untangled) particles in Al6061 matrix, and are presented in **Table 2** and **Figs. 2-5** respectively.

Table 2

Processing techniques of nanocomposites (with different reinforcements pre-processing routes).

Specimen code	Material description	Reinforcement pre-processing		Dispersion routes	Technique (Casting)
		TiO$_2$	MWCNTs		
Al6061	Unreinforced Al6061	-	-	-	
NC1	Al6061 + TiO$_2$ (1 wt%)		-		
HNC1	Al6061 + TiO$_2$ (1 wt%) + MWCNT (0.5 wt%)	Sonication (20 min)		R1 (Presented in **Fig. 2**)	Stir
HNC2	Al6061 + TiO$_2$ (1 wt%) + MWCNT (1 wt%)		Sonication (20 min)		
HNC3	Al6061 + TiO$_2$ (1 wt%) + MWCNT (1.5 wt%)				

HNC4	Al6061 + TiO$_2$ (1 wt%) + MWCNT (1.5 wt%)	Stirred (30 min) + ULP (20 min)	R2 (Presented in **Fig. 3**)	Squeeze (101 MPa)
HNC5		Stirred (30 min) + ULP (20 min) + ball-milling (1 h)	R3 (Presented in **Fig. 4**)	
HNC6		Ball-milling for 6 h	R4 (Presented in **Fig. 5**)	
HNC7				

In Route 1 (R1), an adequate amount of TiO$_2$ and MWCNT nanoparticles were added into acetone and dimethylformamide (DMF) solvents, respectively. Subsequently, the prepared solutions are sonicated individually employing an ultrasonic liquid processor (ULP) having titanium probe (12.5 mm diameter) with pulsed on/off cycles with a duration of 10 sec. for 20 minutes at ambient temperature, to disperse the TiO$_2$ cluster and MWCNT agglomerates. Later, after evaporation of the solvents obtained powders were kept in the vacuum oven at 80 ^{0}C for 72 hours for drying purpose **(Fig. 2)**.
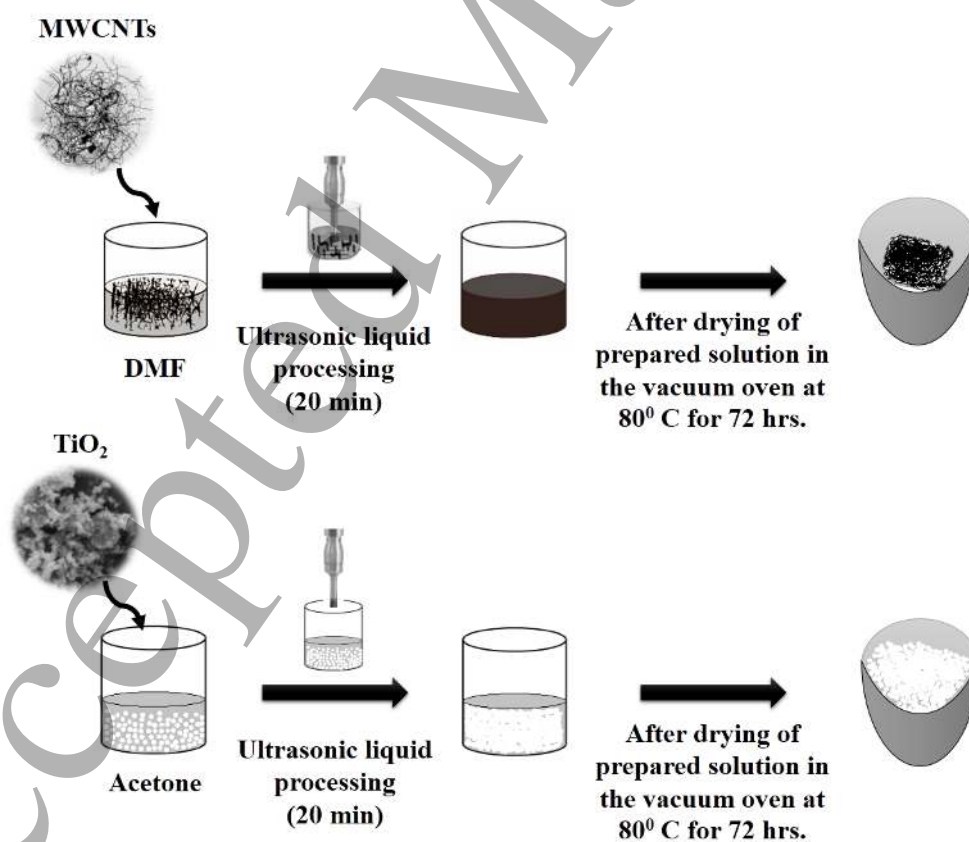
Fig. 2. Schematic of ultrasonic liquid processing of MWCNTs and TiO$_2$ (R1).

In Route 2 (R2), to attain the uniform mixing and dispersion of nanoparticles, 1 wt% of TiO_2 and 1.5 wt% of MWCNTs were added into DMF solvent and stirred exhaustively by using the mechanical shear mixer for 30 min at 500 rpm. Subsequently, the nanoparticles mixture was sonicated for 20 min, followed by drying in a vacuum oven at 80 ^{0}C for 72 hours (**Fig. 3**).
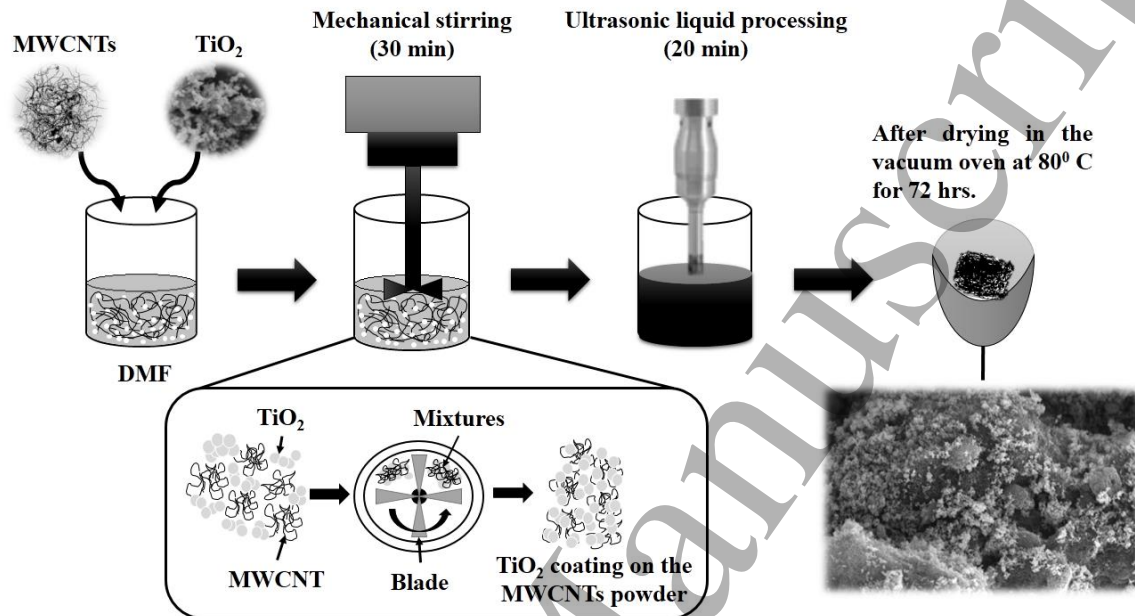

Fig. 3. Schematic of pre-processing of MWCNT-TiO_2 nanoparticles mixture employing R2.

In route 3 (R3), the process involved in route 2 is followed till the drying process, thereafter, to improve the dispersion of nanoparticles, further the nanoparticles mixture was ball-milled using a planetary ball mill at a rotational speed of 200 rpm for 1 hour (at low energy to avoid nanoparticles destruction). The ball-to-powder weight ratio (BPR) was kept at 10:1. The schematic of reinforcement pre-processing R3 is depicted in **Fig. 4.**
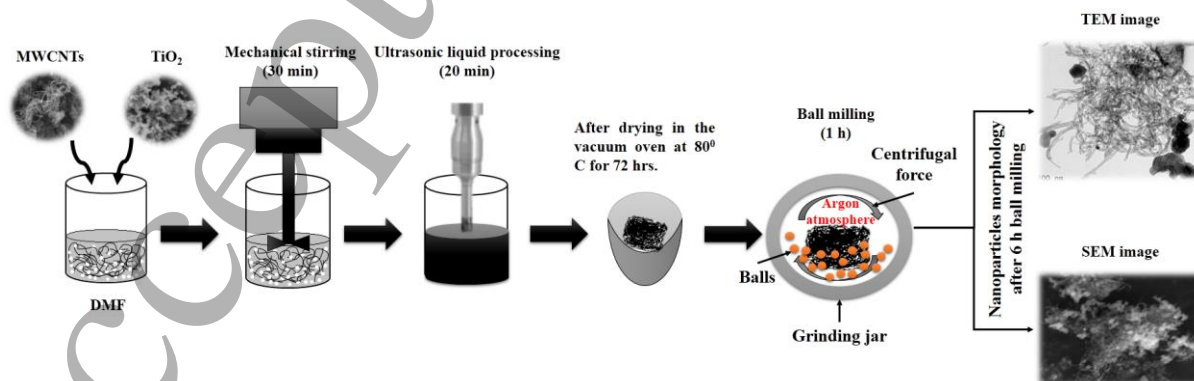
Fig. 4. Schematic of pre-processing of MWCNT-TiO_2 nanoparticles mixture employing R3.

On the other hand, in route 4 (R4) to attain the uniform dispersion of nanoparticles without any destruction in MWCNTs structure, 1 wt% of TiO_2 and 1.5 wt% of MWCNTs were ball-milled in a stainless steel container (without process control agent) at a rotational speed of 200 rpm (low speed) for 6 hours with an interim period of 30 min in every one hour. The schematic illustration of the detailed process is presented in **Fig. 5**.
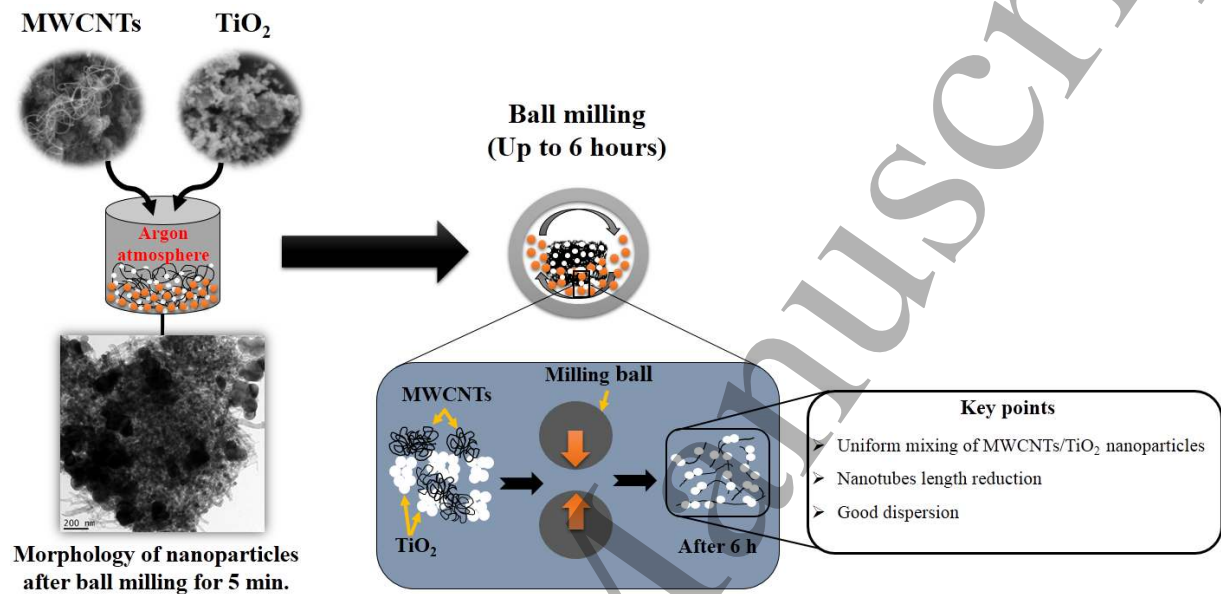

Fig. 5. Schematic of pre-processing of MWCNT-TiO_2 nanoparticles mixture employing R4.

In order to fabricate, Al6061 based nanocomposites reinforced with 1 wt% TiO_2 and 0, 0.5, 1 and 1.5 wt% MWCNTs through ultrasonic-assisted stir/squeeze casting, preheated Al6061 alloy was melted in an electric resistance heating furnace at 850 ^{0}C which consists of an integral mechanical stirrer. The measured amounts of the pre-processed TiO_2 and MWCNT nanoparticles were preheated to 300^0 C for 4 h to remove surface impurities and moisture prior to addition in the aluminum melt. In the present work, preheated reinforcements were appended to Al6061 melt under the argon gas atmosphere by using a combined approach of ultrasonication and optimized mechanical stirring. Further, by opening the bottom stopper of the crucible, the composite slurry was poured into an air-cooled mold to solidify. In squeeze casting, a squeezing pressure of 101 MPa was applied with a holding time of 45 sec during solidification of the composites slurry in cylindrical die. The schematic illustration of the

methodology adopted for the fabrication of ultrasonic-assisted stir/squeeze cast single and hybrid nanocomposites using different reinforcements pre-processing routes are depicted in **Fig. 6**.
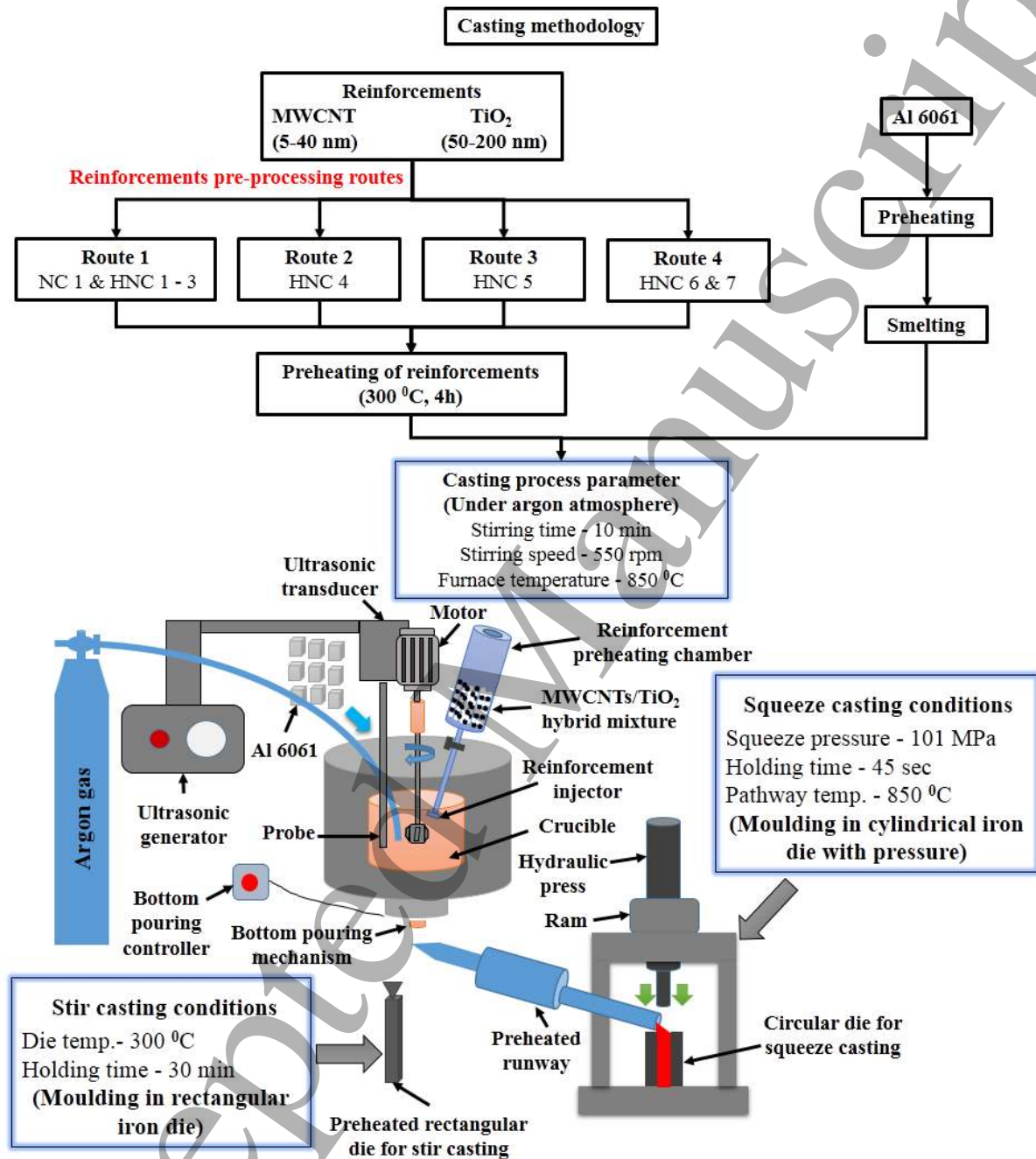

Fig. 6. Schematic illustration of the methodology adopted for the fabrication of specimens through ultrasonic-assisted stir and squeeze casting.

2.2 Material characterization

To characterize the sonicated and ball-milled MWCNTs, pre-processed TiO_2/MWCNT nanoparticle mixtures and stir/squeeze cast nanocomposites various techniques were employed in the present work. The morphology evolution in MWCNTs and TiO_2/MWCNT nanoparticles mixture were analyzed using SEM, Field Emission-SEM, TEM and X-ray diffraction (XRD). SEM examination was performed on EVO 18 research (ZEISS) instrument. Prior to the examination, all the nanoparticles were gold-coated employing a sputter coating instrument. TEM investigations were performed through High Resolution- TEM FEI-Tecnai, G^2 20 Twin instrument at an accelerating voltage of 200 keV. The XRD patterns of nanoparticles and their mixture were obtained through BRUKER D8 Advance X'Pert X-ray diffractometer. In order to analyze the microstructure and grain refinement of the prepared nanocomposites, specimens were prepared using standard metallographic procedures and etched with Keller's reagent. Further, etched specimens were examined employing Zeiss Axio optical microscope. Moreover, to perceive the reinforcements and its dispersal on nanoparticle mixture and as-cast AMMHNCs specimens, EDS and X-ray mapping investigations were performed using SEM equipped with EDX analysis. Further, in order to perform post-failure analysis, the fractured surface of the hybrid nanocomposites was examined employing high-resolution FE-SEM (Thermo Fisher FEI Quanta 250 FEG model).

Subsequently, to investigate the mechanical properties (strengthening) of the stir/squeeze cast Al6061 based hybrid nanocomposites, tensile and hardness tests (Vickers's micro-hardness) were conducted. The tensile test was performed on the INSTRON tensile testing instrument (loaded with 10kN load cell) as per the ASTM E08-8 standards. The UTS of the prepared specimens was evaluated at the crosshead speed of 1.0 mm/min. For each composition, three specimens were tested, and the average value is reported. Prior to tests, all the prepared specimens were polished using a series of silicon carbide emery papers (grit ranges from 220-

2000) in order to eliminate the surface irregularity, as well as defects, from the specimens. The microhardness of the fabricated specimens was measured employing Vickers micro-hardness tester (Matsuzawa, MMT-X series) equipped with optical microscopy under a load of 100 g with a dwell time of 30 s. The diamond indenter was used for testing as well as all experiments were performed according to ASTM: E384-08 standards at ambient conditions [24]. In order to eradicate any chances of error, which may occur during the measurement, the microhardness testing was carried out at twenty different locations on the polished specimens and average values were considered as a final microhardness result.

3. Results and discussion

3.1 Microstructural characterization

In this section, morphological evolution in the MWCNTs and TiO_2/MWCNT mixture with the various pre-processing routes were studied and presented employing SEM, FE-SEM, TEM and XRD. It is a prerequisite to comprehending the influence of different reinforcements pre-processing routes on the physical and mechanical properties of resulting nanocomposites. **Figures 1 (a-b)** show the SEM and TEM images of as-received TiO_2 and MWCNT nanoparticles. It is evident from the images that raw nanoparticles are highly agglomerated in the form of large clusters. In order to fabricate NC1 and HNC1-7, TiO_2 and MWCNT nanoparticles were pre-processed (to achieve uniform dispersion) using various dispersion routes, which are discussed previously in **section 2.1**.

3.1.1 Morphological evolution in the MWCNTs with the sonication and ball-milling time

It is found that the dispersion techniques/time strongly influences the nanotubes morphology and structural characteristics (aspect ratio). Hence, prior to the reinforcement, the effect of sonication and ball-milling time on MWCNTs microstructure was investigated. In order to examine the morphological evolution in the MWCNTs with the dispersion time, a certain

amount of MWCNTs are sonicated in DMF solvents for 5-40 min under an ice bath condition. Further, after drying, dispersion uniformity and morphology of the MWCNTs were investigated using SEM (**Fig. A.1**) (**Appendix**) and TEM (**Figs. 7 and 8**). From **Figs. A.1 and 7**, it is observed that, as the sonication time increases up to 20 min, the MWCNT clusters split into untangled ropes, and distinct MWCNTs are observed. From these findings, it is evident that the dispersion uniformity of the MWCNTs increases with increasing the sonication time up to 20 min.
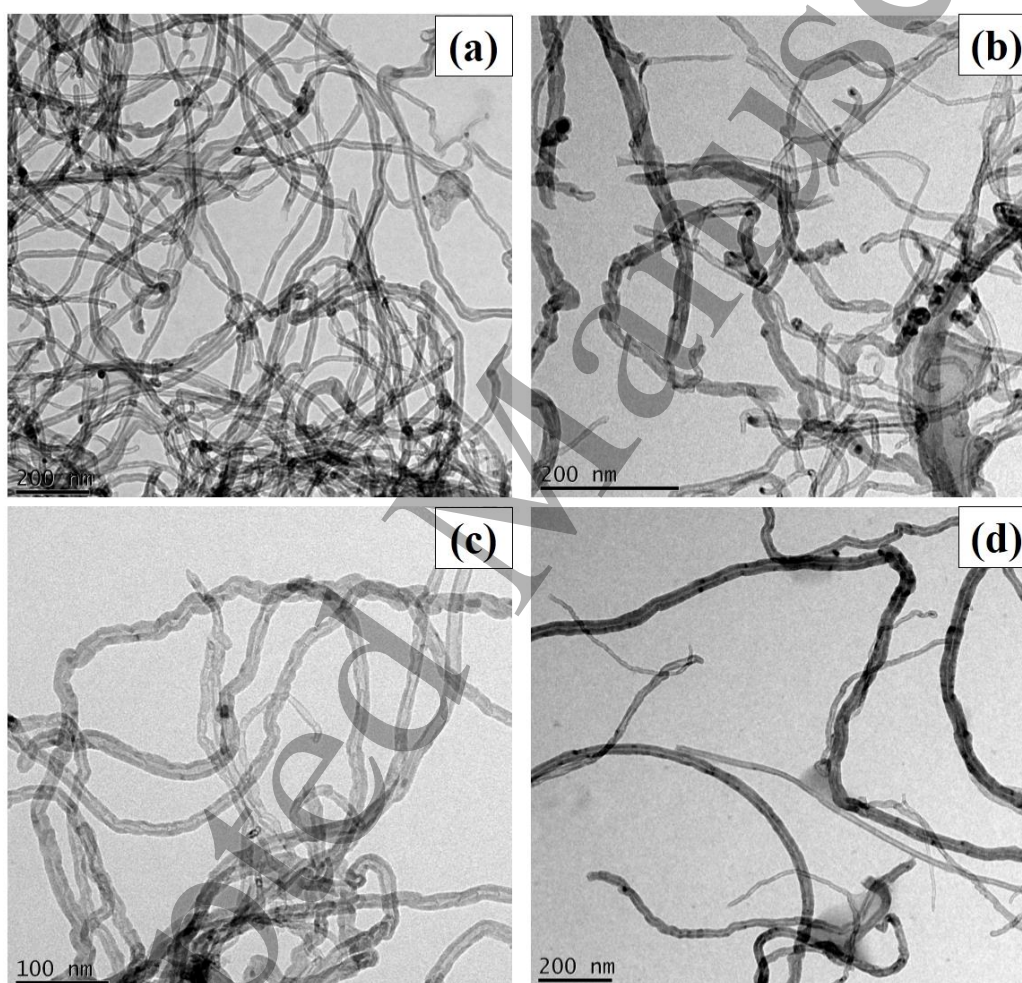

Fig. 7. TEM images depicting the morphology of the MWCNTs dispersed by sonication for (a) 5, (b) 10, (c) 15, and (d) 20 min.

Figures 8 (a-d) show the TEM images of MWCNTs dispersed by sonication for the 25, 30 and 40 minutes. From **Figs. 8 (a-c)**, it can be seen that the nanotubes dispersed for 25 and 30 minutes show some MWCNT bonding and junctions (indicated by a red arrow) that lead to the development of nanotubes agglomerates. HR-TEM image, in **Fig. 8 (c),** confirms the presence

of MWCNT junctions and the merging of MWCNTs. Further, with an increase in sonication time up to 40 min, the achieved dispersion with short sonication time is lost, and dense MWCNT agglomerates were observed, as shown in **Fig. 8 (d)**. Microstructure investigation of MWCNTs dispersed for a duration of up to 20 min does not exhibit such bonding of nanotubes. Hence, it can be concluded from the above observation that the 20 min of sonication is sufficient to disperse the MWCNTs.
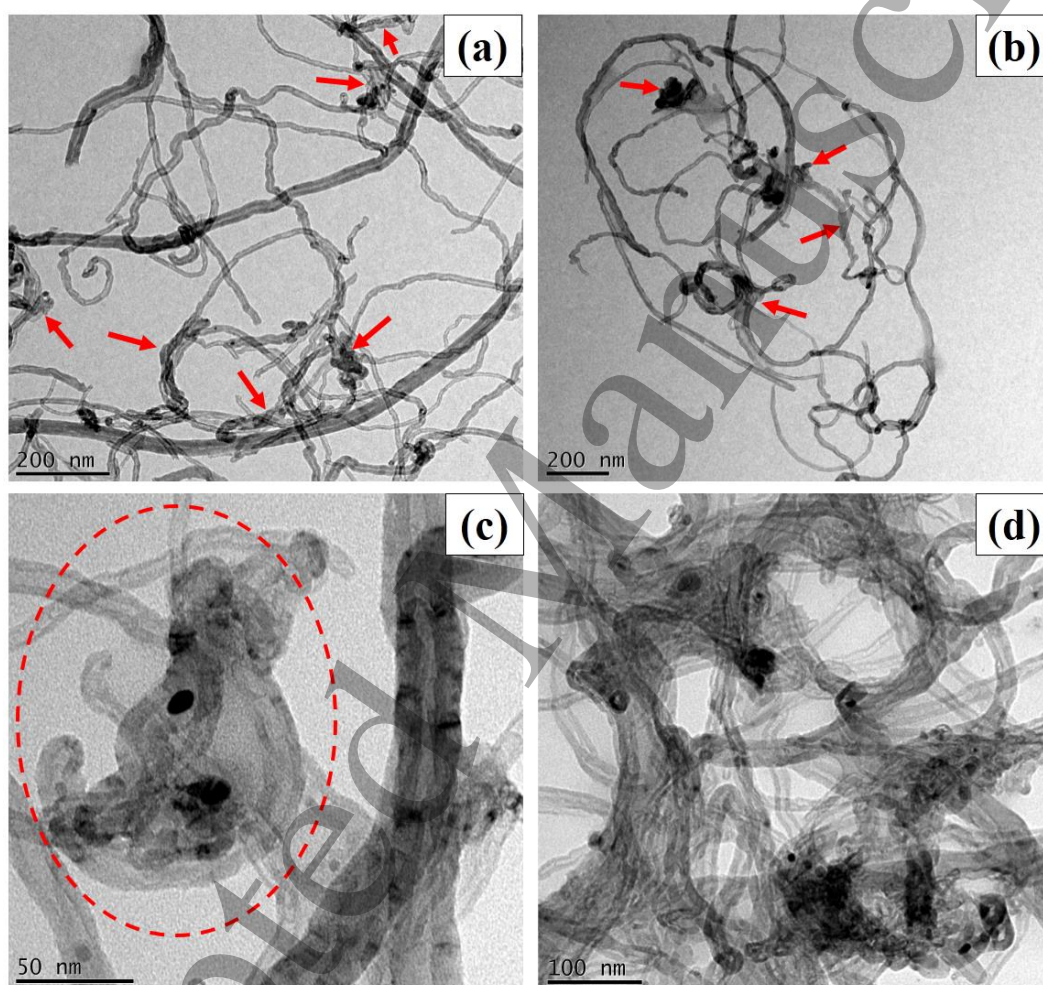

Fig. 8. TEM images of the MWCNTs dispersed by sonication for (a) 25, (b) 30, (c) 30 (high magnification) and (d) 40 min.

In order to examine the influence of ball-milling time on the MWCNTs microstructure, an adequate amount of MWCNTs were milled with a rotational speed of 200 rpm for the duration of up to 6 h in an argon atmosphere. **Figure 9** shows the morphological evolution in the MWCNTs for 5 min to 6 h ball-milling time using TEM images. It can be observed from these images that as the ball-milling time increases, the MWCNT agglomerates are untangled and

distinct nanotubes are perceived without destruction in its structure, as shown in **Figs. 9 (a-e)**.

Apart from this, by increasing milling time up to 6 h, MWCNTs shortening (change in aspect

ratio) can be clearly observed due to the shearing effects of balls and is presented in **Fig. 9 (f)**.
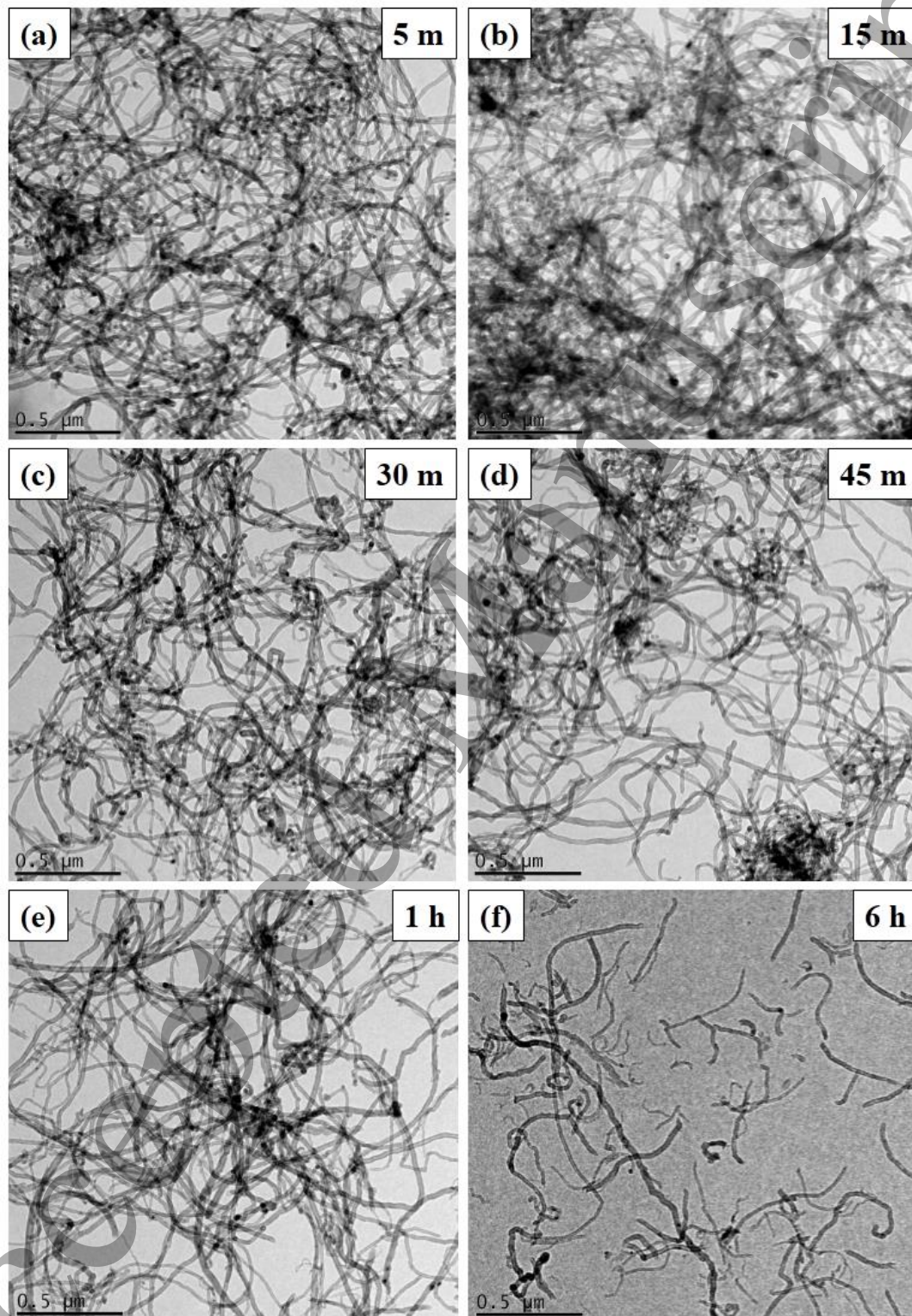
Fig. 9. TEM images of the MWCNTs dispersed by ball-milling for (a) 5 min, (b) 15 min, (c) 30 min, (d) 45 min, (e) 1 h and (f) 6 h.

The variation in the outer diameter of MWCNTs subjected to increasing ball-milling time was also studied using ImageJ software and presented in **Fig. A.2 (Appendix).** From these images it can be observed that the ball-milling process causes an increase in the number of small diameters of MWCNTs for 5, 15, 30, 45, 60 min and 6 h, resulting in lower average diameters of 20.91, 18.32, 18.06, 18.01, 15.21 and 14.53 nm respectively. These findings suggest the accomplishment of uniform dispersion during the ball-milling process [17].

3.1.2 Morphological evolution in the MWCNT/TiO$_2$ mixture dispersed by different pre-processing routes

Figure 10 shows the SEM images of the MWCNT/TiO$_2$ mixture dispersed by R2. It can be clearly observed from these images that the stirring ensures the mixing of TiO$_2$/MWCNT nanoparticles, while sonication breaks the large clusters of nanoparticles into small ones but still, MWCNT agglomerates are clustered with TiO$_2$ nanoparticles due to insignificant dispersion (shown in enlarged view). **Figure 11** depicts the FE-SEM image of the nanoparticles mixture, in which the presence of individual MWCNT was clearly observed in the TiO$_2$ cluster, due to sonication duration of 20 min.
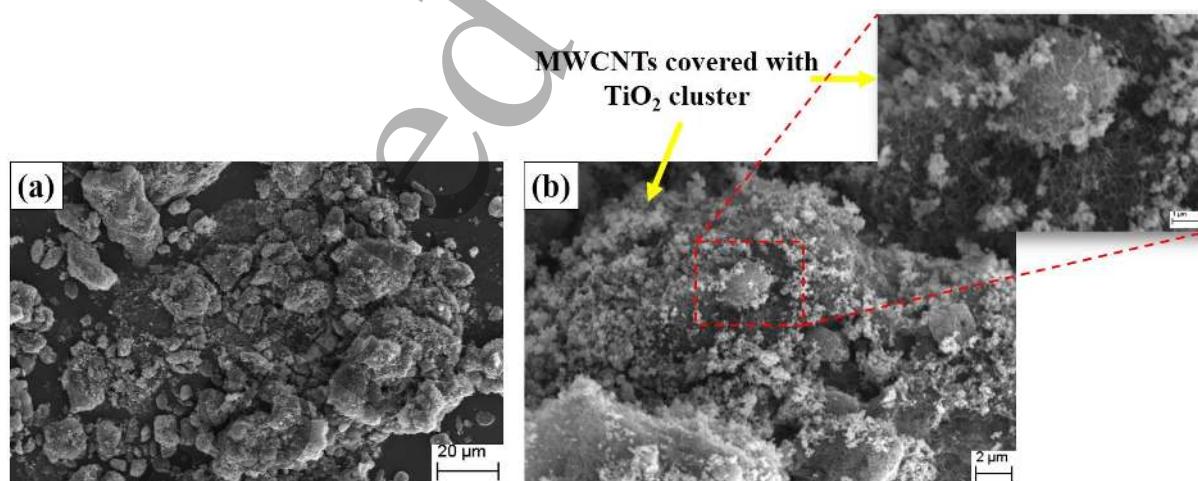

Fig. 10. SEM images of MWCNT-TiO$_2$ nanoparticles mixture dispersed by R2) (a) low magnification, and (b) high magnification.
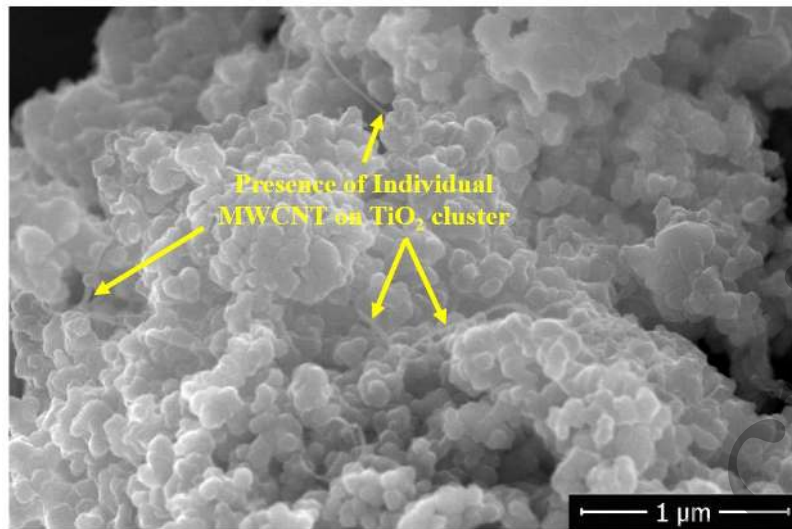
Fig. 11. FE-SEM image of the MWCNT-TiO$_2$ nanoparticles mixture dispersed by R2 depicting the presence of individual MWCNTs on the TiO$_2$ cluster.

Figures 12 and 13 show the SEM and TEM images of the MWCNT/TiO$_2$ nanoparticles mixture dispersed by R3. The particle size distribution (PSD) of pre-processed MWCNT/TiO$_2$ nanoparticles by employing R3 demonstrates the reduction in the size of the clusters of the nanoparticles mixture as compared to reinforcement pre-processing R2, due to ball-milling process (as presented in **Fig. 14**). During the ball-milling process, MWCNT cluster and nano-size TiO$_2$ particles collided aggressively when they passed between the balls, and owing to that detachment of MWCNT and TiO$_2$ nanoparticles from their agglomerates were observed (**Fig. 13a**). **Figures 12 (b)** and **13 (b)** show the high magnification SEM and TEM images of MWCNT/TiO$_2$ mixture, in which a reduction in the size of MWCNT agglomerates and TiO$_2$ cluster are evident, but still MWCNT agglomerates are clustered with few TiO$_2$ nanoparticles, which results in non-uniform dispersion of MWCNT/TiO$_2$ nanoparticles.
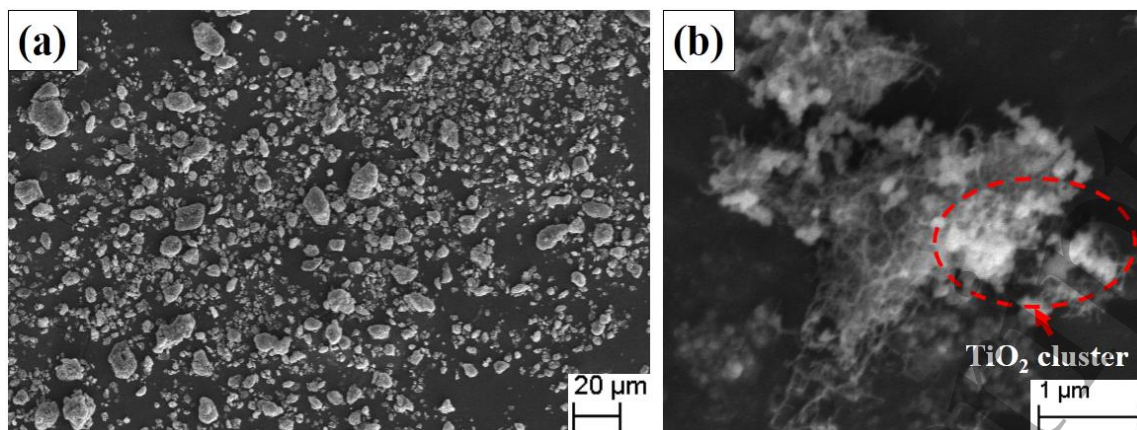
Fig. 12. SEM images of MWCNT-TiO$_2$ nanoparticles mixture dispersed by the R3.
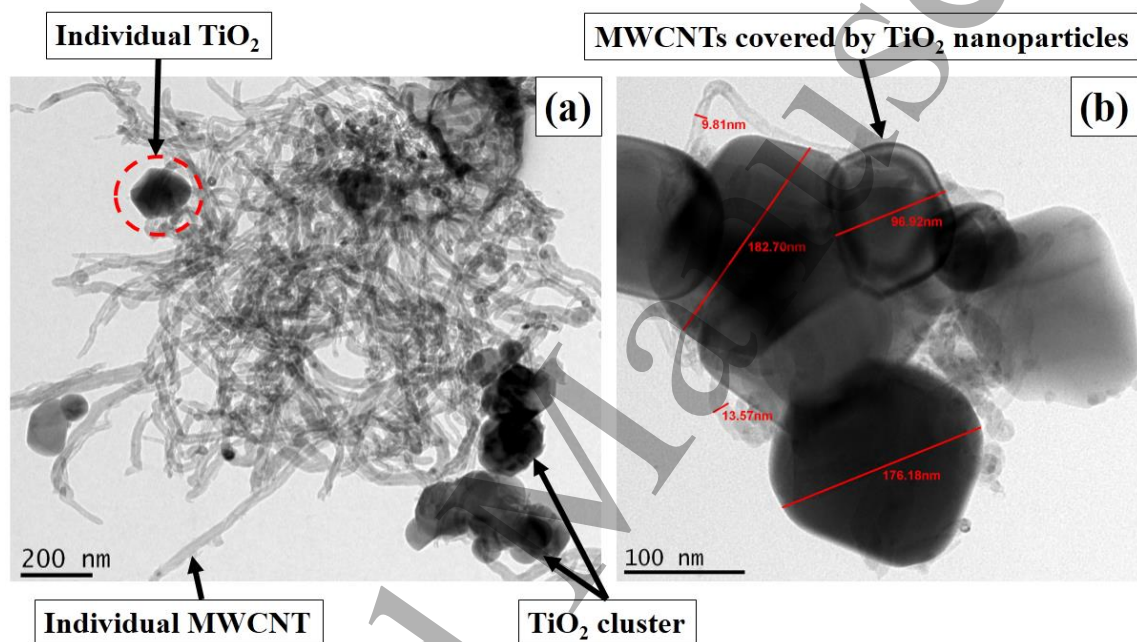
Fig. 13. TEM images of MWCNT-TiO$_2$ nanoparticles mixture dispersed by the R3.
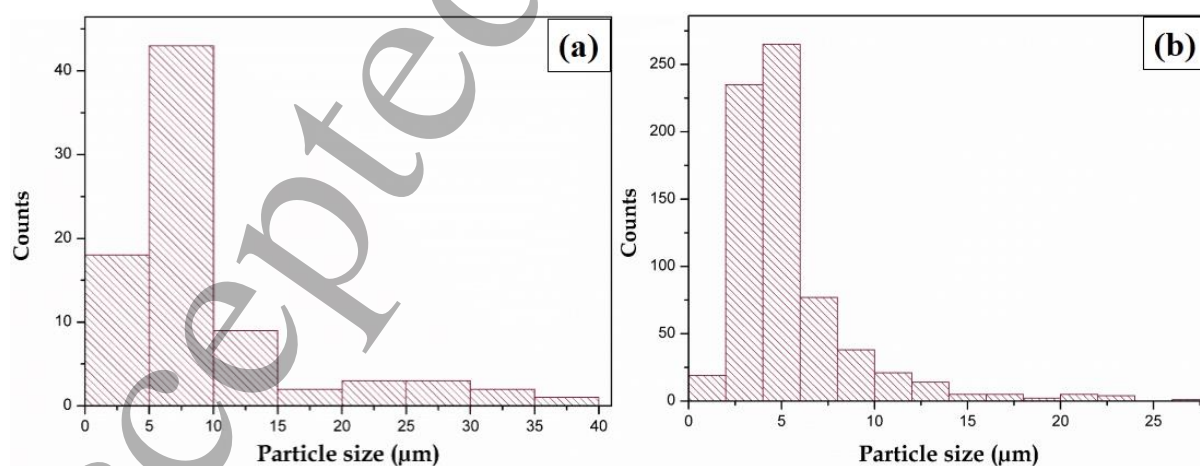
Fig. 14. PSD of MWCNT-TiO$_2$ nanoparticles mixture dispersed by (a) R2 and (b) R3.
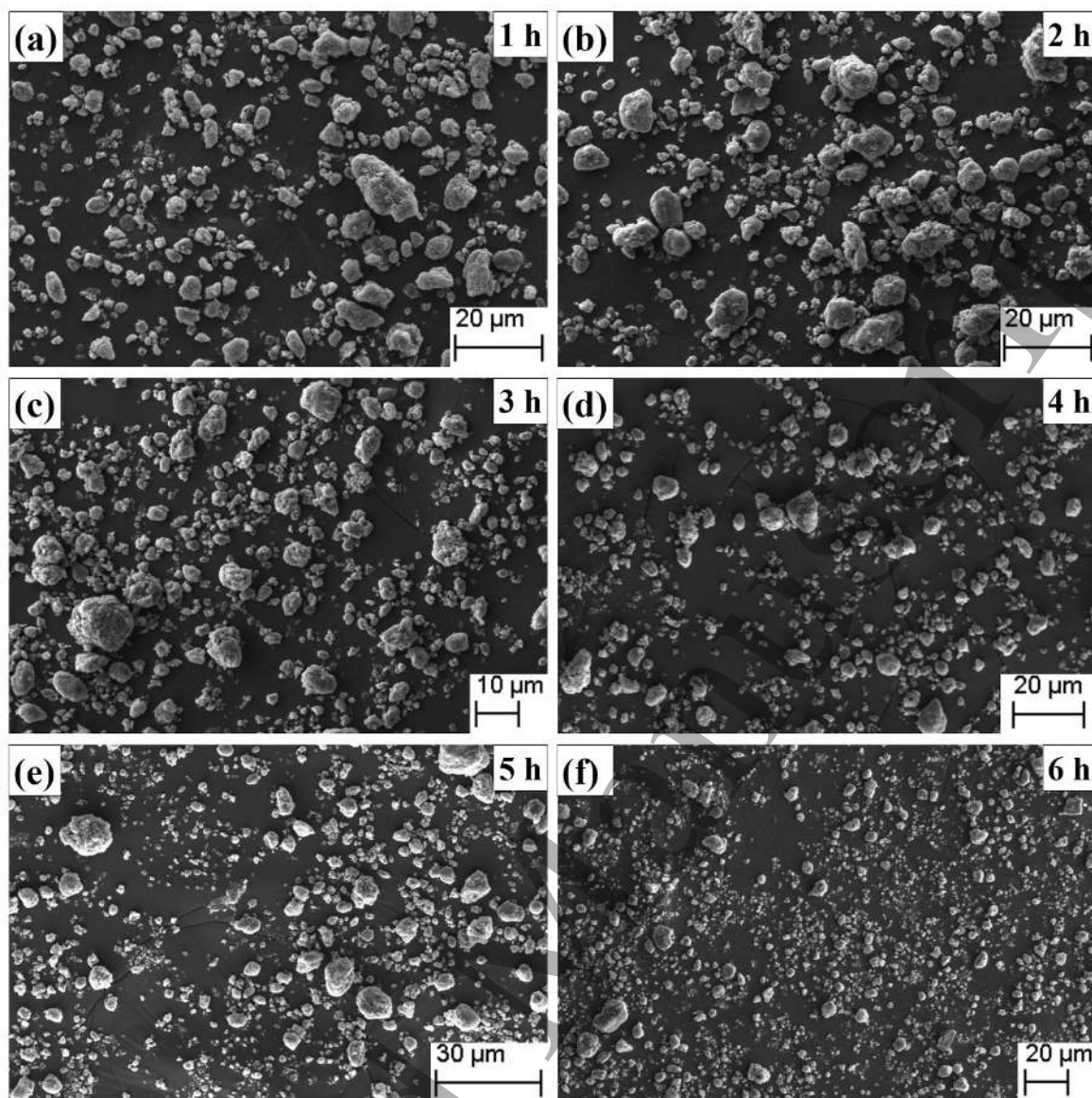
Fig. 15. Low magnification SEM images of the MWCNT-TiO$_2$ nanoparticles mixture ball-milled for different times (a) 1 h, (b) 2 h, (c) 3 h, (d) 4 h, (e) 5 h, and (f) 6 h.

Figure 15 shows the morphologies of the MWCNT/TiO$_2$ mixture for different ball-milling times. It can be observed from images that the particle size of the nanoparticles mixture decreased as the duration of the ball-milling increases from 1 h to 6 h (avg. particle size is presented in **Fig. 16**), which is mainly due to the shearing effects of the balls. It is also found that nanoparticles mixture (ball-milled for 1 h) has an average particle size of 5.54 µm, and after 6 h milling particle size reduces to 3.88 µm. This confirms that the 6 h ball-milling decreases the particle size of the MWCNT/TiO$_2$ nanoparticles mixture.
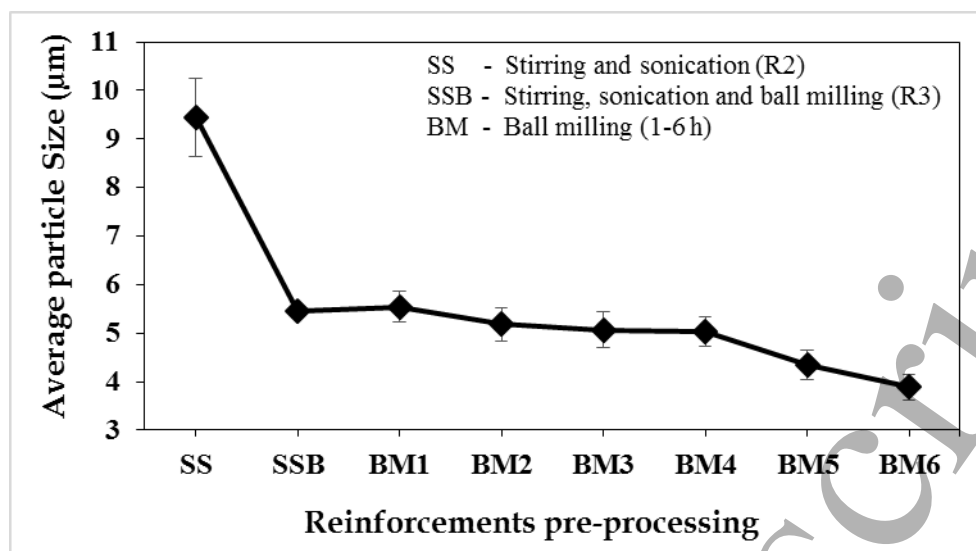
Fig. 16. Particle size (avg.) of MWCNT-TiO$_2$ nanoparticles mixture dispersed by different pre-processing routes (R2-R4).

The homogeneity and nanoparticles dispersion was examined by using high magnification SEM images exploration (**Fig. 17**). From these images, it can be observed that the cluster size of the TiO$_2$ nanoparticles was decreased as the ball-milling time increases, and gradually dispersed into the MWCNT nanoparticles. When the ball-milling duration was comparatively short (1-3 h), the large TiO$_2$ clusters adhered to the surface of MWCNT agglomerates (**Figs. 17a-c**). Subsequently, upon increasing the ball-milling duration to 5 h, the size and quantity of the TiO$_2$ cluster reduced, even a few individual MWCNT were also observed (**Fig. 17e**). After 6 h of ball-milling, very few TiO$_2$ clusters were observed over the short length MWCNTs, as shown in **Fig. 17 (f)**, similar results were also presented earlier in **Fig. 5** with the aid of schematic. It illustrates, at the beginning stage of ball-milling, the mixture comprises large agglomerates of TiO$_2$ and MWCNT nanoparticles. Further, as the milling time increases, MWCNTs were shortened [34] and TiO$_2$ clusters were broken into small clusters (having few TiO$_2$ nanoparticles) or individual TiO$_2$ nanoparticle owing to the shearing effect of the balls, as presented in **Fig. 18 (a)**.
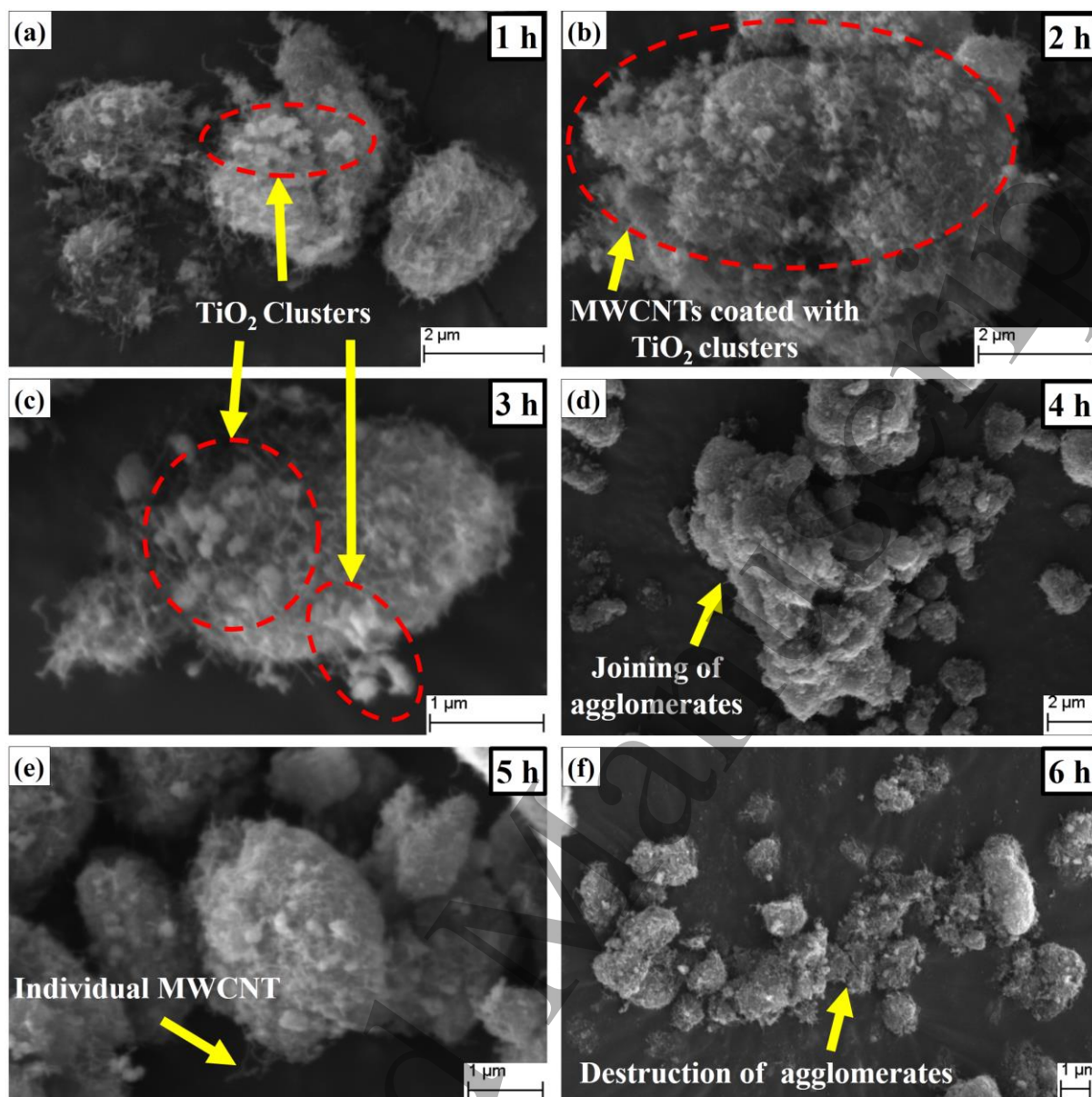
Fig. 17. SEM images showing the influence of milling time on the dispersion of MWCNT-TiO$_2$ nanoparticles mixture for (a) 1 h, (b) 2 h, (c) 3 h, (d) 4 h, (e) 5 h, and (f) 6 h.

Moreover, not any deterioration in MWCNTs structure has been perceived during detailed HR-TEM investigation of the TiO$_2$/MWCNT nanoparticles mixture (**Fig. 18b).** Thus, based on the microstructure investigation, it is found that during 6 h ball-milling, intensive compressive and shear stresses were imposed on the nanoparticle mixture, which helps to de-agglomerate nanoparticle clusters into few or distinct ones.
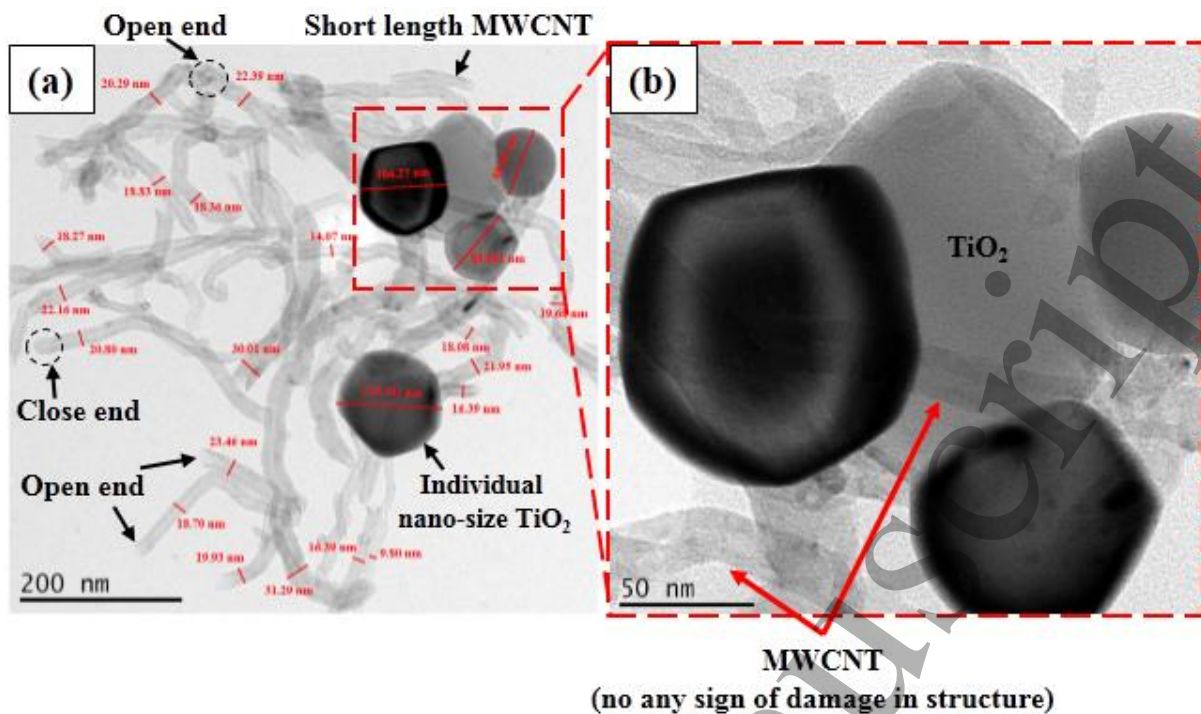
Fig. 18. TEM images of the 6 h ball-milled MWCNT-TiO$_2$ nanoparticles mixture.

EDX spectrum with the selected-area diffraction (SAD) pattern of the nanoparticle mixture is presented in **Fig. A.3 (Appendix),** which shows various rings and diffraction spots, confirming the presence of TiO$_2$ and MWCNT nanoparticles. The typical diffraction pattern in **Fig. A.3** (inside) corresponds to the MWCNTs in the TiO$_2$/MWCNT nanoparticles mixture. **Figure A.4 (Appendix)** shows the HR-TEM images of the 6 h ball-milled MWCNT/TiO$_2$ nanoparticles mixture, which shows interlayer spacing of 0.353 nm and 0.349 nm in TiO$_2$ and MWCNTs, respectively [31,35,36]. During the HR-TEM investigation of nanoparticles, no destruction in MWCNT and TiO$_2$ structure were observed.

XRD plot of as-received MWCNTs, TiO$_2$ and their pre-processed mixture are presented in **Fig. 19**. XRD pattern of nanoparticle mixture demonstrated the C (002), C (110), C (101), TiO$_2$ (101), TiO$_2$ (004), TiO$_2$ (200), TiO$_2$ (105), TiO$_2$ (211), TiO$_2$ (204), TiO$_2$ (116), TiO$_2$ (220) and TiO$_2$ (215) miller indices for various intensity of peak. The crystallite size of the TiO$_2$ nanoparticles and pre-processed MWCNTs/TiO$_2$ mixture are presented in **Table 3.** MWCNTs/TiO$_2$ mixture dispersed by R4 demonstrates a reduced crystallite size than the

mixture dispersed by R2 and R3, which is in agreement with the TEM results. From **Fig. 19**, it can be found that the intensity of TiO_2 peaks is reduced in 6 h ball-milled mixture due to the reduction in the crystallite size and de-clustering of TiO_2 (anatase) nanoparticles [35,37].
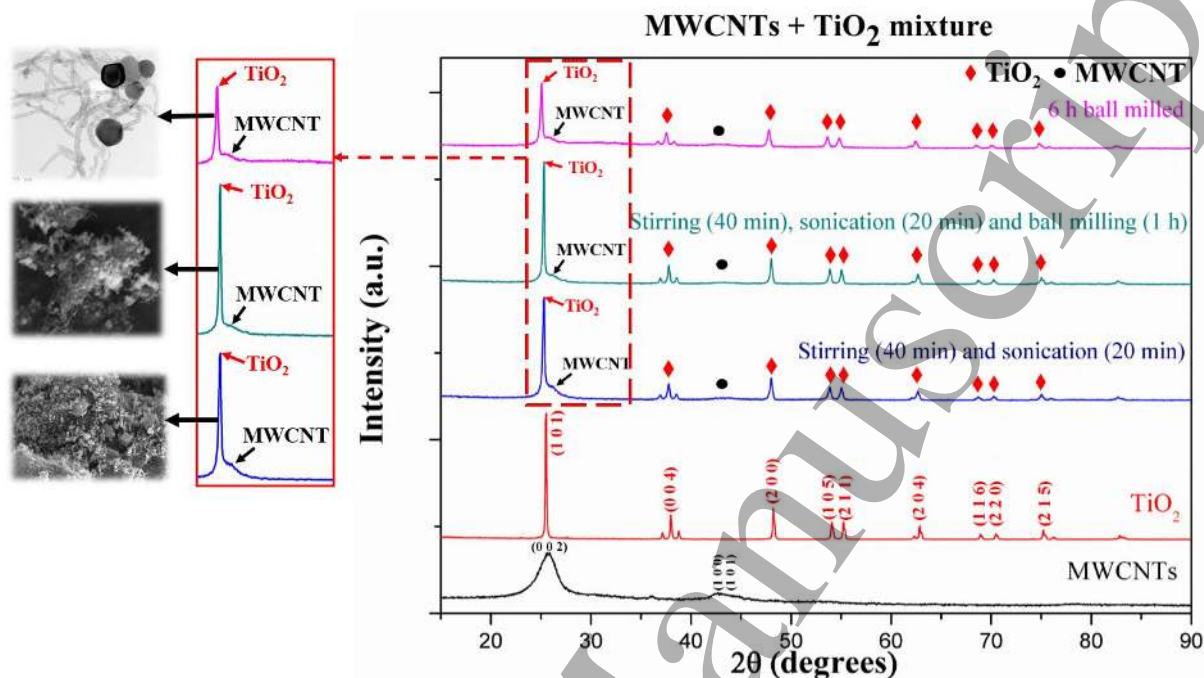

Fig. 19. XRD patterns of MWCNTs, TiO_2 and MWCNT-TiO_2 nanoparticles mixture dispersed by R2, R3 and R4.

Table 3

Crystallite size of the nanoparticles/mixture determined by XRD

Sample	Crystallite size (nm)
TiO_2 nanoparticles	53
Stirred (30 min) + sonication (20 min) {R2}	37
Stirred (30 min) + sonication (20 min) + ball-milling (1 h) {R3}	45
Ball milling (6 h) {R4}	29

3.1.3 SEM-MAP and optical micrograph of the specimens

Microstructure (SEM-MAP) examination of the NC1, HNC4, HNC5 and HNC6 are presented in **Figs. 20 (a-d).** It is difficult to recognize any noteworthy difference in the microstructure of the NC1, HNC4, HNC5 and HNC6 in the SEM images (inside). However, from EDS and elemental maps, the presence and dispersal of C, Ti and O in fabricated specimens are observed.
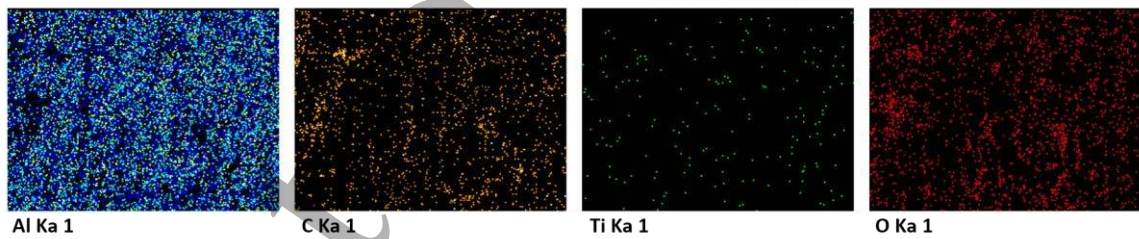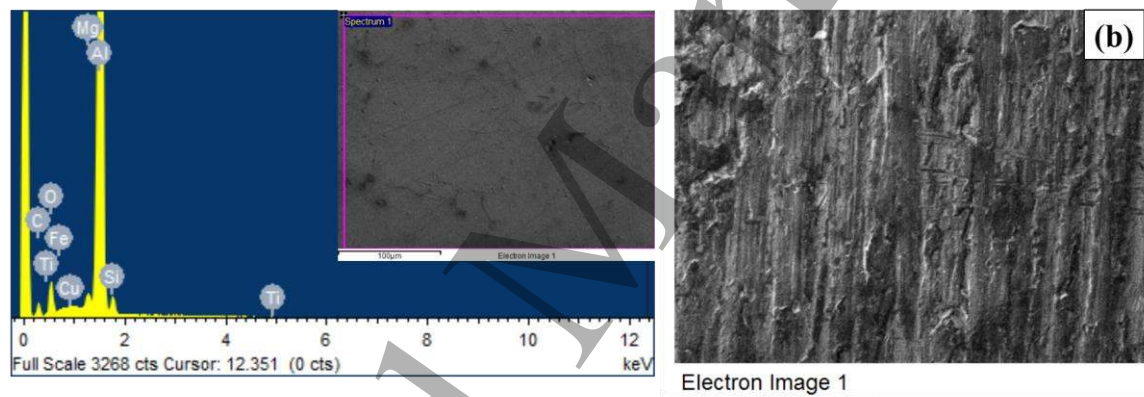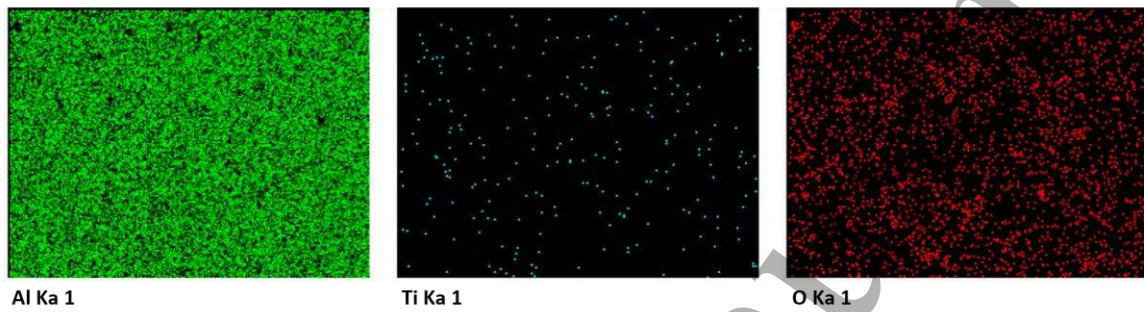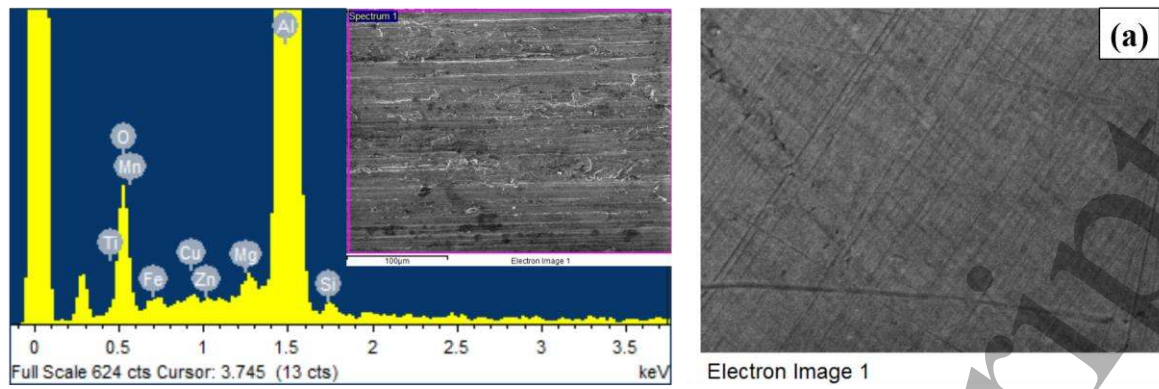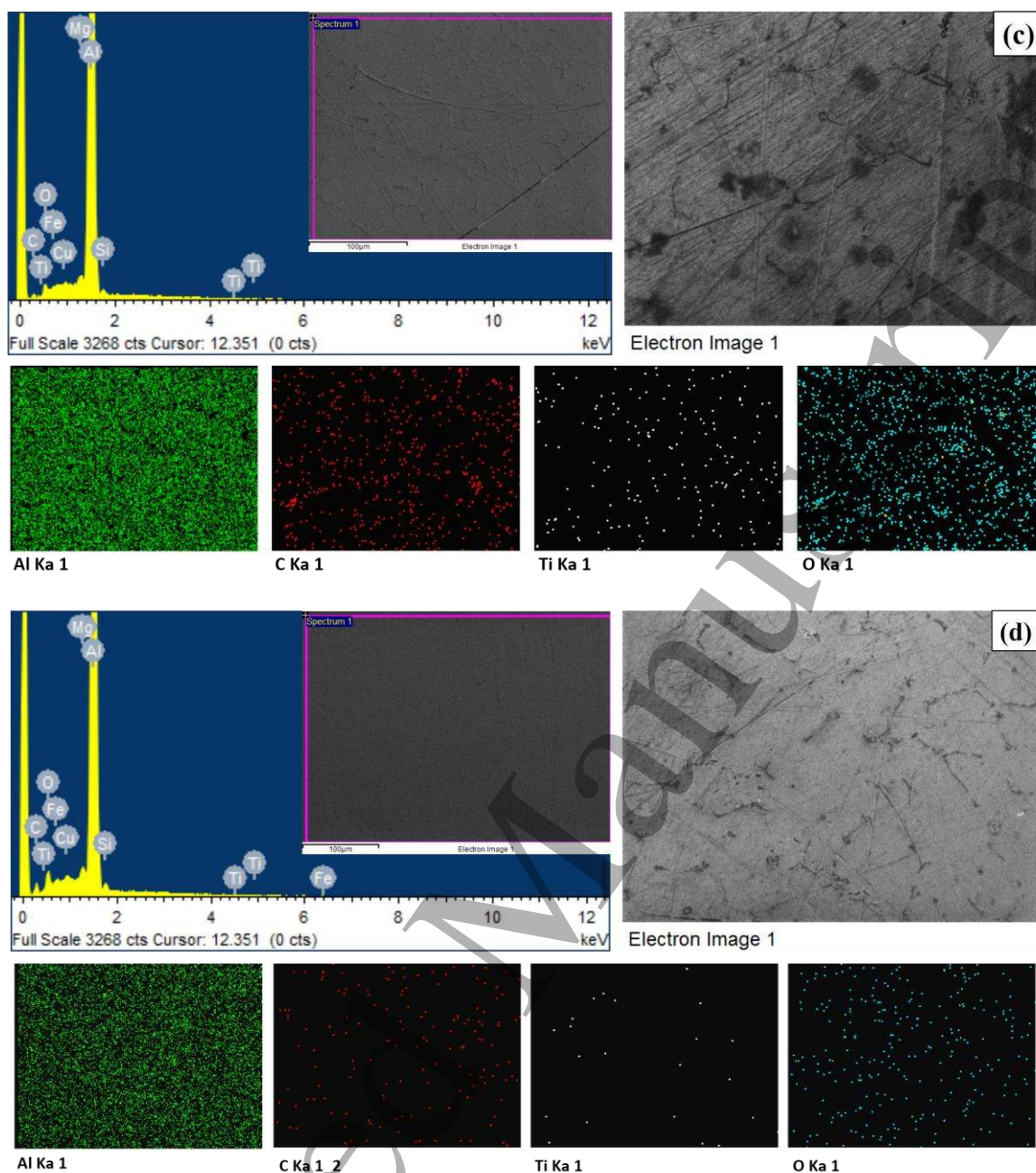
Fig. 20. SEM-MAP analysis of (a) NC1, (b) HNC4, (c) HNC5 and (d) HNC6.

Figures 21 (a-i) show the optical micrographs of the ultrasonic-assisted stir cast NC1 and hybrid nanocomposites (HNC1-7). It is observed from OM images of hybrid nanocomposites that with the increase in MWCNT reinforcement in HNC1, HNC2 and HNC3, the MWCNTs start to agglomerate owing to insufficient dispersion and mixing. The size of the MWCNT agglomerates was increased to 2.31, 2.58 and 4.66 µm in HNC1, HNC2 and HNC3, respectively, with the enhancement in MWCNTs content from 0.5, 1 and 1.5 wt% as shown in **Figs. 21 (c-e**). Subsequently, by adopting reinforcements pre-processing R2, MWCNT

agglomerates size reduces to 2.18 µm in HNC4 (**Fig. 21f**). However, by using reinforcement pre-processing R3 much smaller size of MWCNT agglomerates is attained in HNC5 (**Fig. 21g**). Further, reinforcement of TiO_2/MWCNT nanoparticles mixture by using reinforcements pre-processing R4 results in uniform dispersion of nanoparticles in the Al6061 matrix, which efficiently restrains grain growth by grain boundary pinning [35]. It should be noted that by employing reinforcements pre-processing routes (R2-R4), the PSD of the nanoparticles mixture reduces (presented in **Fig. 16**), causing a significant reduction in the size of MWCNT agglomerates. Grain refinement is evident in the optical micrographs of stir cast NC1 and hybrid nanocomposites as compared to unreinforced Al6061 due to thermal mismatch, strengthening imposed by TiO_2/MWCNT nanoparticles and ultrasonic-assisted casting approach [21,24,38]. Further, due to applied squeezing pressure, the gap among the dendrites was unceasingly getting shortened, which results in the attainment of uniform microstructure and more ultra-grain refinement in squeeze cast HNC7 (**Fig. 21i**) [39].
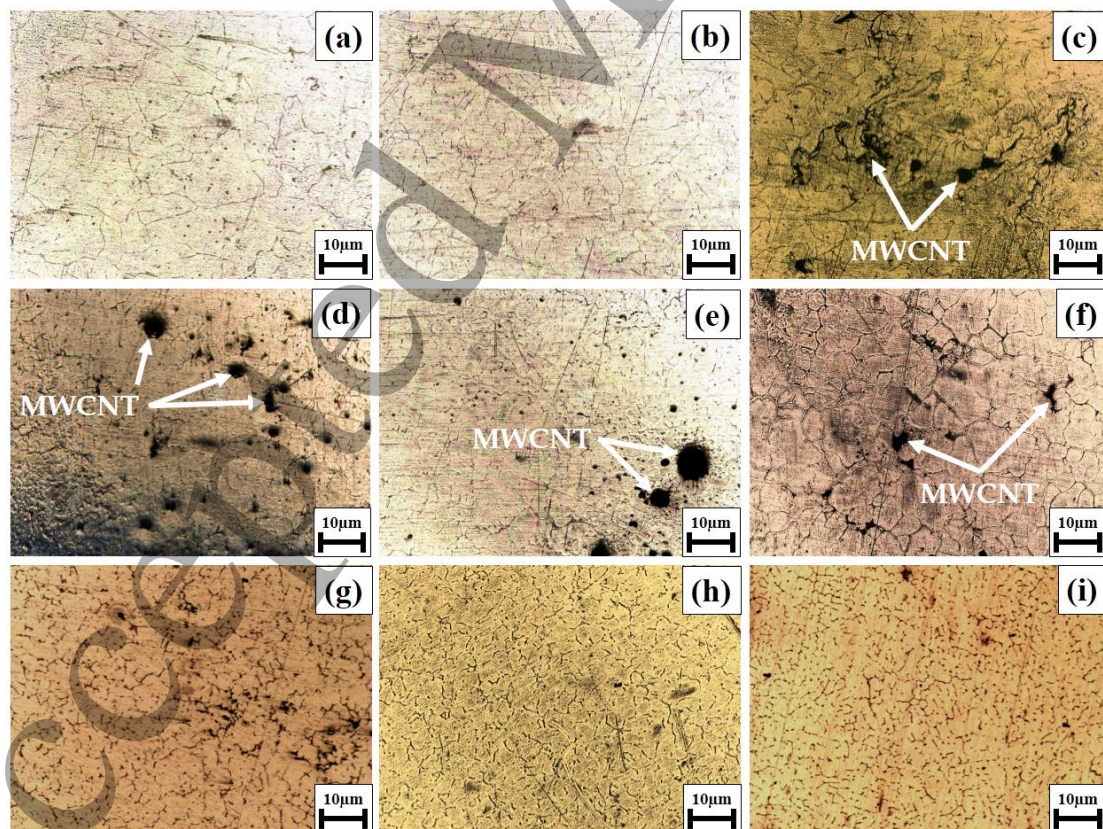

Fig. 21. Optical micrographs of (a) as-cast Al6061, (b) NC1, (c) HNC1, (d) HNC2, (e) HNC3, (f) HNC4, (g) HNC5, (h) HNC6 and (i) HNC7.

3.2 Physical and mechanical properties investigation

3.2.1 Density and % porosity

Theoretical density, experimental density and percentage porosity of as-cast Al6061, NC1 and hybrid nanocomposites (HNC1-7) are presented in **Fig. 22.** Al6061, TiO_2 and MWCNTs used in the present work having density values of 2.7 g/cm^3, 4.2 g/cm^3 and 2.1 g/cm^3, respectively. For the evaluation of the theoretical density of prepared specimens, the rule of mixtures (ROM) was used [40], which can be represented as

$$\rho_{th} = \rho_m W_m + \rho_r W_r \qquad (1)$$

Where

W_m and W_r - weight fractions of the matrix and reinforcement;

ρ_m and ρ_r - density of matrix and reinforcement;

ρ_{th} = theoretical density of the specimen under investigation

The experimental density (ρ_{exp}) of the as-cast Al6061, NC1 and HNC1-7 were investigated at ambient conditions by using water immersion displacement method as per the ASTM C135–2003 standards employing a precision digital electronic weighing balance of 0.0001 g accuracy [27].

Further, the percentage porosity of the prepared specimens was determined by using the following relation

$$\% \, porosity = \frac{\rho_{th} - \rho_{exp}}{\rho_{th}} \qquad (2)$$

The increase in the theoretical density of NC1 over the as-cast Al6061 is due to the higher weight fraction of TiO_2 nanoparticles. Further, a decrease in the theoretical density of hybrid nanocomposites (HNC1-7) as compared to NC1 is due to the reinforcement of low-density MWCNTs. As compared to theoretical density, the lower experimental density of the NC1 and

hybrid nanocomposites is mainly due to porosity. The porosity of prepared specimens is usually associated with nanoparticle agglomeration, poor wettability characteristics, shrinkage during solidification and clustering of reinforcements in the melt [41]. From **Fig. 22** it can be found that the experimental density of NC1, HNC1, HNC2 and HNC3 is decreased owing to nanoparticles agglomeration [42]. Further, upon employing reinforcements pre-processing routes 2, 3 and 4, enhancement in experimental density and decrement in percentage porosity of the HNC4, HNC5, HNC6 and HNC7 were observed, due to the attainment of homogenous dispersion and uniform mixing of TiO_2/MWCNT nanoparticles mixture into the matrix. It is also evident from these results that the higher percentage porosity of the HNC1-3 is associated with non-uniform dispersion and inadequate mixing of TiO_2/MWCNT nanoparticles in Al6061 melt, which can be significantly reduced by employing reinforcements pre-processing approaches (R2-R4) prior to its addition in the matrix.
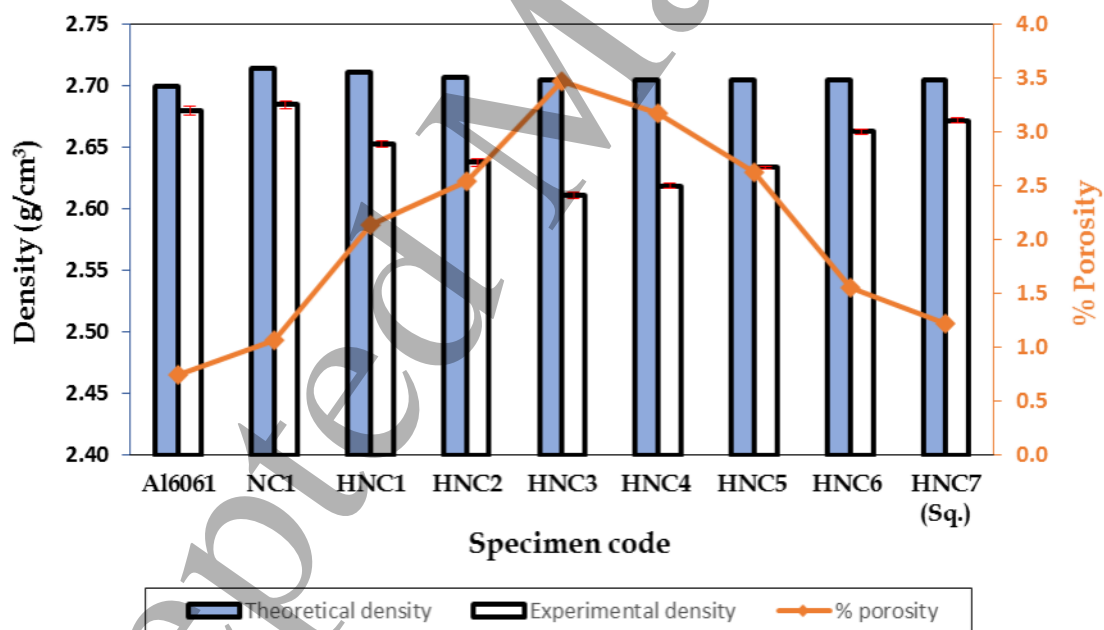
Fig. 22. Theoretical and experimental densities of as-cast Al6061, NC1 and hybrid nanocomposites.

3.2.2 Mechanical properties

The enhanced mechanical properties of AMMHNCs are significantly important for their wide-ranging applications in aircraft and automobile fields. The stress-strain curves of the as-cast

Al6061, NC1 and hybrid nanocomposites (HNC1-7) are presented in **Fig. 23**. It was evident from the figure that the reinforcement of TiO_2/MWCNT nanoparticles has a significant effect on the mechanical properties of the resulting nanocomposites. As compared to as-cast Al6061, NC1 and hybrid nanocomposites (HNC1-HNC7) exhibit lesser elongation (lower ductility) but demonstrate superior UTS and YS (as shown in **Fig. 24**).
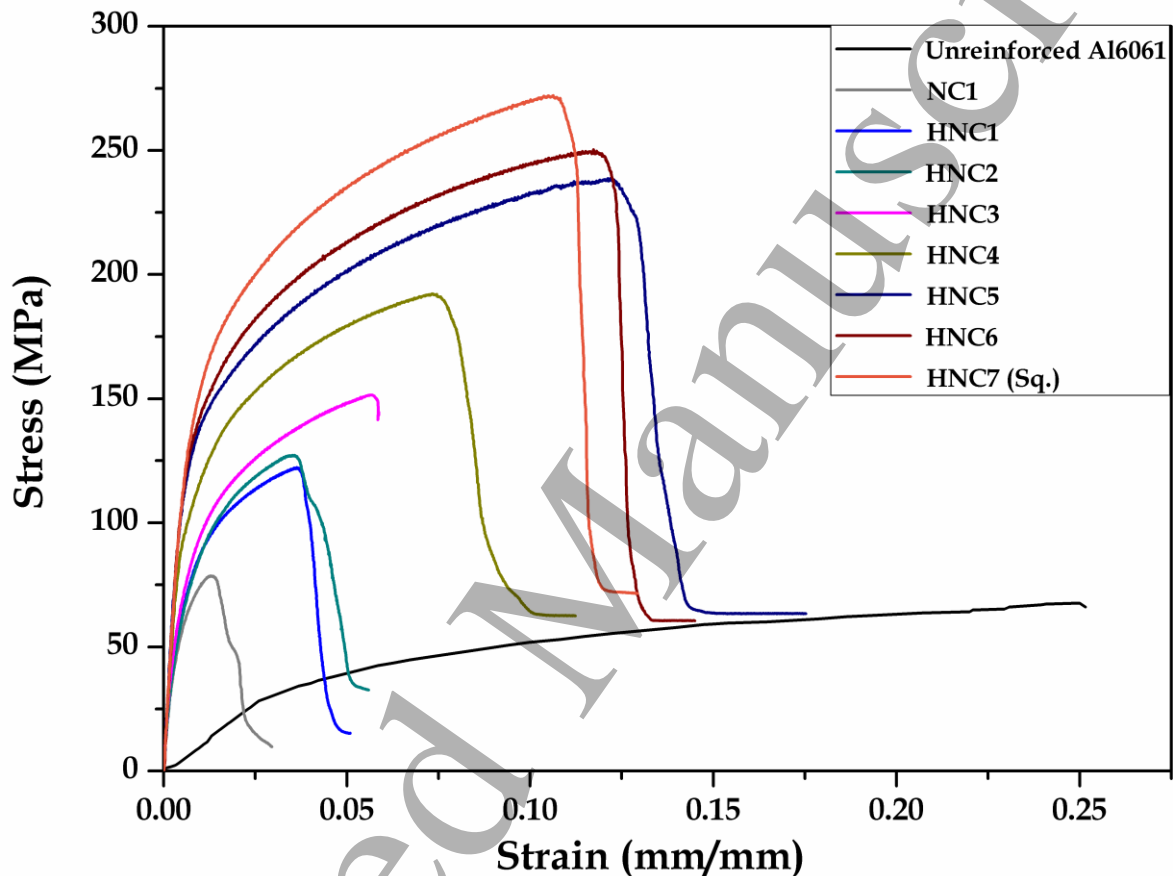
Fig. 23. Stress-strain plot of as-cast Al6061, NC1 and hybrid nanocomposites (HNC1-7).

The elongation of NC1 reduced due to the reinforcement of nano-sized TiO_2 particles. This reduction in elongation of NC1 over the Al6061 is due to the non-deformable behavior of TiO_2 nanoparticles, which renders the deformation of Al6061 [21,43]. Further, reinforcement of TiO_2/MWCNT nanoparticles into the Al6061 by using reinforcement pre-processing R1, R2 and R3 shows that the elongation of hybrid nanocomposites increases as compared to elongation of NC1 due to nanoparticles agglomeration and weak bonding among the matrix and reinforcements. Subsequently, reinforcement of 6 h ball-milled TiO_2/MWCNT

nanoparticles into the Al6061 matrix demonstrates a reduction in the elongation of HNC6 as compared to HNC5, which is associated with a uniform dispersion of nano-reinforcements and reduction in the hybrid nanocomposites molecular mobility [44]. The decrease in elongation of HNC6 as compared to Al6061 is deliberated in detail in **section 3.3**. Moreover, lower elongation of HNC7 as compared to HNC6 is associated with the attainment of uniform microstructure and more ultra-grain refinement.
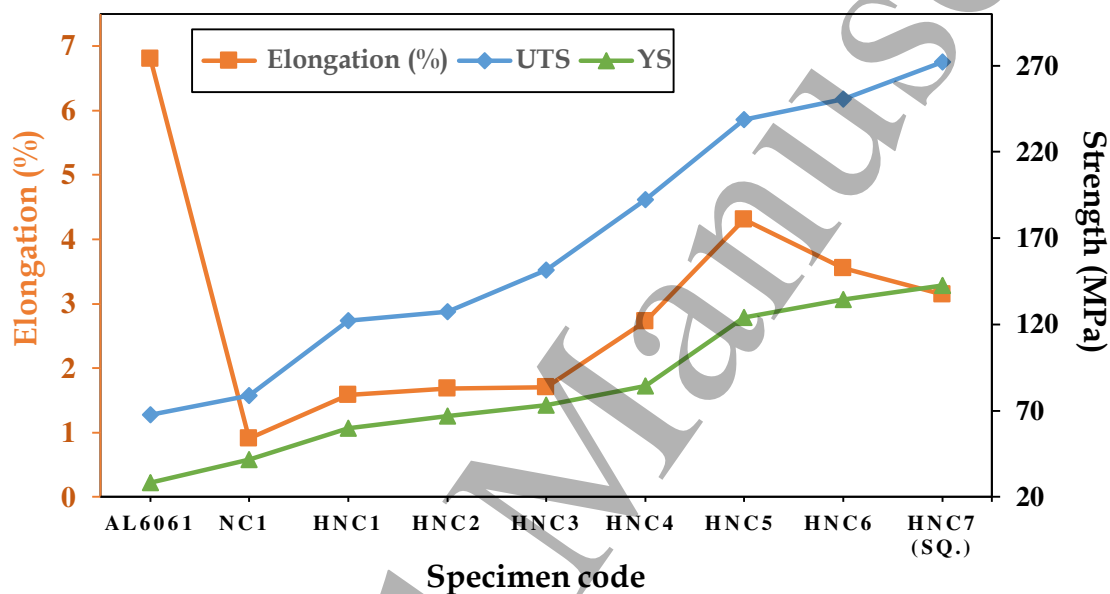
Fig. 24. Variation of elongation, YS and UTS of as-cast Al6061, NC1 and hybrid nanocomposites (HNC1-7).

The YS and UTS of the NC1 and hybrid nanocomposites increases over the as-cast Al6061, due to the reinforcement of TiO_2 and TiO_2/MWCNT nanoparticles respectively. It is found that the YS enhances by 45.71% for NC1, 109.94% for HNC1, 135.46% for HNC2, 157.37% for HNC3, 196.59% for HNC4, 335.53% for HNC5, 371.59% for HNC6 and 400.22% for HNC7 compared to as-cast Al6061. Subsequently, improvement of UTS for NC1, HNC1, HNC2, HNC3, HNC4, HNC5, HNC6 and HNC7 compared to as-cast Al6061 are 16.15 %, 80.65 %, 87.89 %, 123.81 %, 183.91 %, 252.76 %, 269.75 % and 301.86 % respectively. It was observed that the UTS, YS and microhardness of HNC1 were higher by 55.54%, 44.08% and 8.43%,

respectively, as compared to NC1 due to the presence of secondary reinforcement (0.5wt% MWCNTs). The above-stated improvement in the mechanical properties of HNC1 as compared to NC1 confirms the influence of secondary reinforcements in the matrix. Furthermore, effective reinforcement of nano-size TiO_2/MWCNT particles in the matrix by using pre-processing R4 and ultrasonic-assisted casting, causing significant enhancement in the tensile strength of HNC6. The increased strength of the HNC6 as compared to HNC3 is mainly due to MWCNTs shortening (change in the aspect ratio of MWCNTs), reduction in percentage porosity and homogenous dispersion of nano-size TiO_2/MWCNT particles. Further, about 8.68 % and 301.86 % higher UTS were observed in the squeeze cast HNC 7 as compared to HNC6 and Al6061, which shows good agreement with the results obtained in the literature [39]. Based on these outcomes, it can be observed that the increased strength of the NC1 and hybrid nanocomposites are associated with grain refinement, nanoparticle strengthening and load sharing executed by nanoparticles [27,45].

3.2.3 Microhardness

The variations in microhardness values of the ultrasonic-assisted stir/squeeze cast Al6061, NC1 and hybrid nanocomposites (HNC1-HNC7) are presented in **Fig. 25**. Microhardness of the fabricated specimens is increased due to the addition of TiO_2 and TiO_2/MWCNT nanoparticles in the base Al6061 matrix. The improvement of microhardness for NC1, HNC1, HNC2, HNC3, HNC4, HNC5, HNC6 and HNC7 compared to as-cast Al6061 are 10 %, 19.27 %, 20.89 %, 30.72 %, 33.04 %, 35.36 %, 50.28 % and 77.82 % respectively. The improved microhardness of NC1 over the Al6061 is due to the presence of nano-sized TiO_2 nanoparticles, which enhances the dislocation density and slow down the dislocation motion [21,45]. Further, stir cast hybrid nanocomposites prepared by using reinforcement pre-processing R1 and R2 shows nominal enhancement over the Al6061 owing to nanoparticle agglomeration and are in good agreement with the optical micrograph investigations.

Subsequently, the microhardness of 103.70 HV was achieved in the case of HNC6 prepared by using reinforcement pre-processing R4. The highest hardness value of 122.20 HV was attained in squeeze cast HNC7. These squeeze cast hybrid nanocomposites are 17.84% and 77.82% harder than the stir cast HNC6 and as-cast Al6061, respectively. The improvements in the microhardness of prepared specimens are owing to the combined effect of nanoparticle strengthening effects, grain size refinement and thermal mismatch strengthening imposed by nano-sized TiO_2/MWCNT particles [33,39].
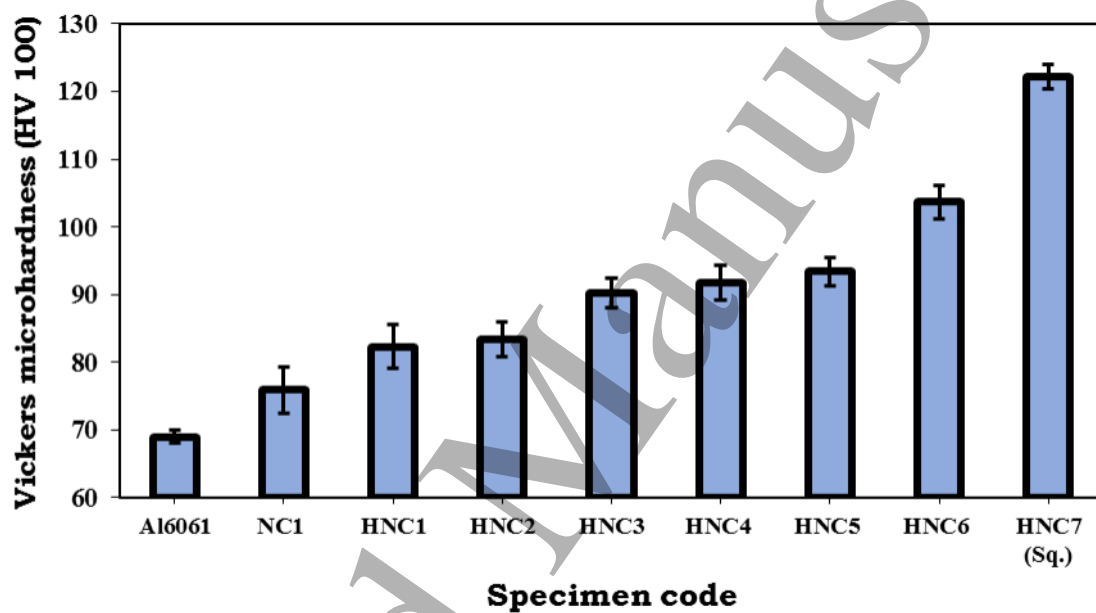

Fig. 25. Microhardness of as-cast Al6061, NC1 and hybrid nanocomposites (HNC1-7).

Results obtained from the tensile tests are consistent with the microhardness tests and confirm the influence of TiO_2/MWCNT reinforcements for NC1 and hybrid nanocomposites fabricated through ultrasonic-assisted stir/squeeze casting techniques. These results exhibit that the reinforcements of nano-size ceramic and nanomaterial enhance the mechanical properties of resulting single and hybrid nanocomposites, but to utilize the utmost properties of reinforcements their uniform dispersion within the matrix is mandatory. In the present investigation, by using different reinforcement pre-processing routes, progressive augmentation in the mechanical properties of the hybrid nanocomposites were achieved.

Numerous mechanisms might have involved in enhancing the mechanical properties of the prepared specimens, which are deliberated one by one as follows. Firstly, the reinforcement (dispersion strengthening) of the uniformly dispersed TiO_2/MWCNT nanoparticles mixture with the perfect structure in Al6061 restricts the movements of dislocations in the matrix according to Orowan mechanism [46]. Secondly, the effective interfacial bonding among the Al6061 matrix and TiO_2/MWCNT nanoparticles permits a smooth transfer of load to the particles. Lastly, the improvement in the mechanical properties of NC1 and hybrid nanocomposites are associated with refined grain structure according to Hall-Petch theory [27]. Hence, the improved mechanical properties of the ultrasonic-assisted stir/squeeze cast hybrid nanocomposites are associated with the combined effect of Hall-Petch and Orowan mechanisms, and it was clearly observed from the grain refinement of NC1 and hybrid nanocomposite (**Figs. 21b-i**) as compared to Al6061 (**Fig. 21a**). Moreover, the increase in the wt% of MWCNT nanoparticles and employment of different reinforcements pre-processing routes further increases the influence of the above factors, which results in an additional increase in the mechanical properties.

It was observed that the tensile strength of HNC4, HNC5 and HNC6 was higher by 22%, 58% and 65%, respectively, as compared to HNC3. While, the microhardness of HNC4, HNC5 and HNC6 was higher by 1.78%, 3.55%, 15% respectively over the HNC3. This improvement is associated with effective reinforcement of TiO_2/MWCNT nanoparticles mixture in the matrix by using reinforcement pre-processing route R2, R3 and R4. Subsequently, squeeze cast HNC7 shows an enhancement in UTS and microhardness of about 9% and 18% respectively over stir cast HNC6. Lower elongation and improved microhardness were observed for NC1 and hybrid nanocomposites over the Al6061, which is mainly due to the reinforcement of hard ceramic and nanomaterial (TiO_2 and MWCNTs) nanoparticles into the matrix and exhibits a similar trend as reported by other researchers [21].

3.3 Fractography

The strengthening of the nanocomposite is closely interconnected to the interfacial bonding among the matrix and reinforcement materials. **Figures 26-28** show the fractured surface morphology (SEM and FE-SEM images) of Al6061-TiO$_2$-MWCNT nanocomposites comprising various percentages of nano-size reinforcements, after tensile testing at ambient atmosphere.
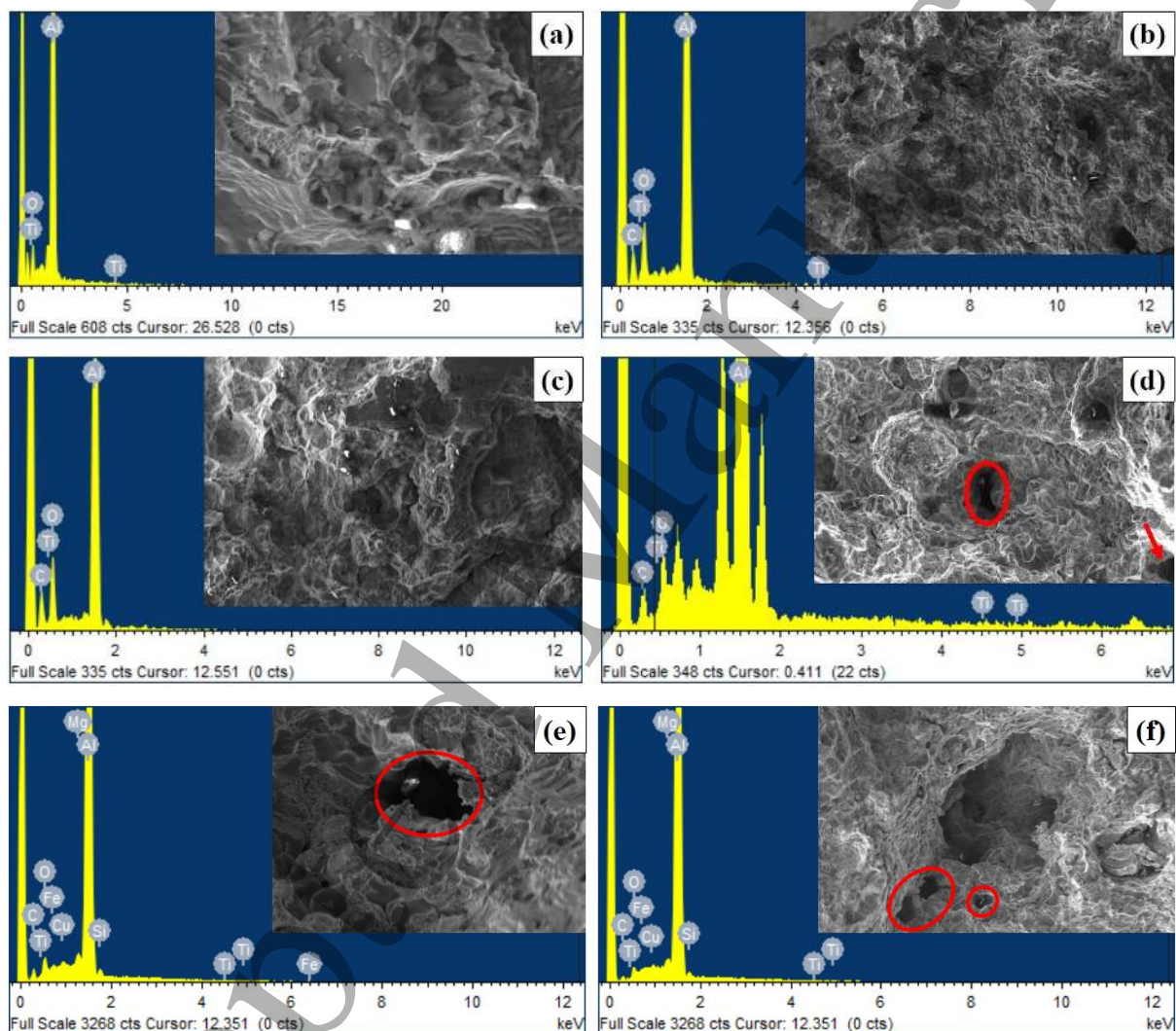
Fig. 26. EDX with fracture area (inside) of (a) NC1, (b) HNC1, (c) HNC2, (d) HNC3, (e) HNC4 and (f) HNC5.

Figures 26 (a-f) shows EDX with the fracture area (inside) of NC1, HNC1, HNC2, HNC3, HNC4 and HNC5. In **Figs. 26 (a-f)** peaks of reinforcements (Ti, O and C) is evident and confirming the addition of MWCNTs and TiO$_2$ nanoparticles. **Figures 26 (a-c)** shows the fracture surface morphology of NC1, HNC1 and HNC2, which demonstrates that the dimples

present on the nanocomposites are not deep as in the fracture surface of Al6061 [24,47]. This is mainly due to relatively less percentage elongation of nanocomposites than that of as-cast Al6061 (**Fig. 24**). Subsequently, the fracture surface of HNC3-5 (**Figs. 26d-f**) comprises large empty pockets. The occurrence of such empty pockets might be due to the agglomeration of nano-reinforcements and possibly signify the location of nanoparticle clusters. The nanoparticle clusters were towed out all together beyond a particular load and abridged the area for supporting the tensile stress [21]. Therefore, the lower UTS was observed for HNC3-5 over the HNC6. The same is also observed in the high-magnification FE-SEM image of HNC3 and presented in **Fig. 27 (d)**. Further, high-magnification SEM images of tensile tested specimens of Al6061-TiO$_2$ (1 wt%)-MWCNT (0–1.5 wt%) hybrid nanocomposites demonstrates that the NC1 (**Fig. 27a**) and HNC1-3 fracture surface (**Figs. 27b-d**) comprises large clusters of TiO$_2$ and TiO$_2$/MWCNT nanoparticles due to insufficient mixing and dispersion of reinforcements. This agglomeration is the evidence of the development of cracks from nanoparticles and matrix interface **(Fig. 27d)**.
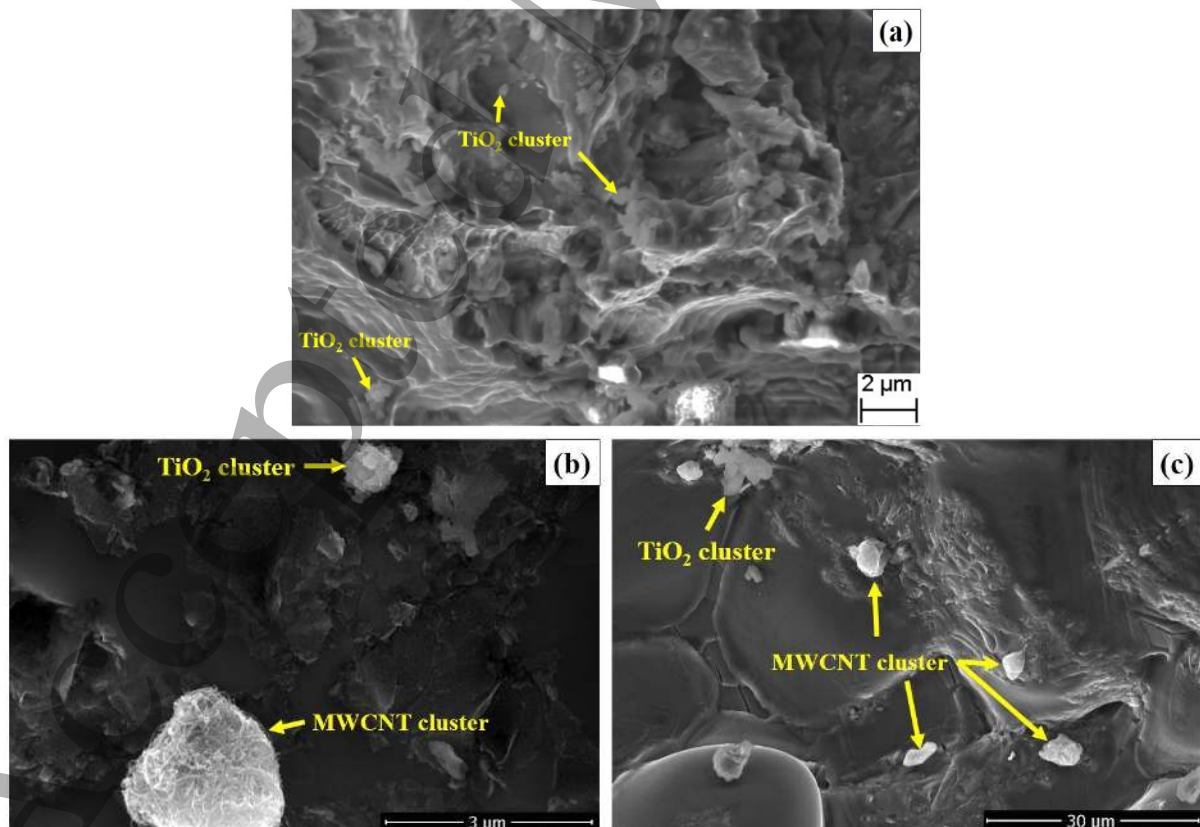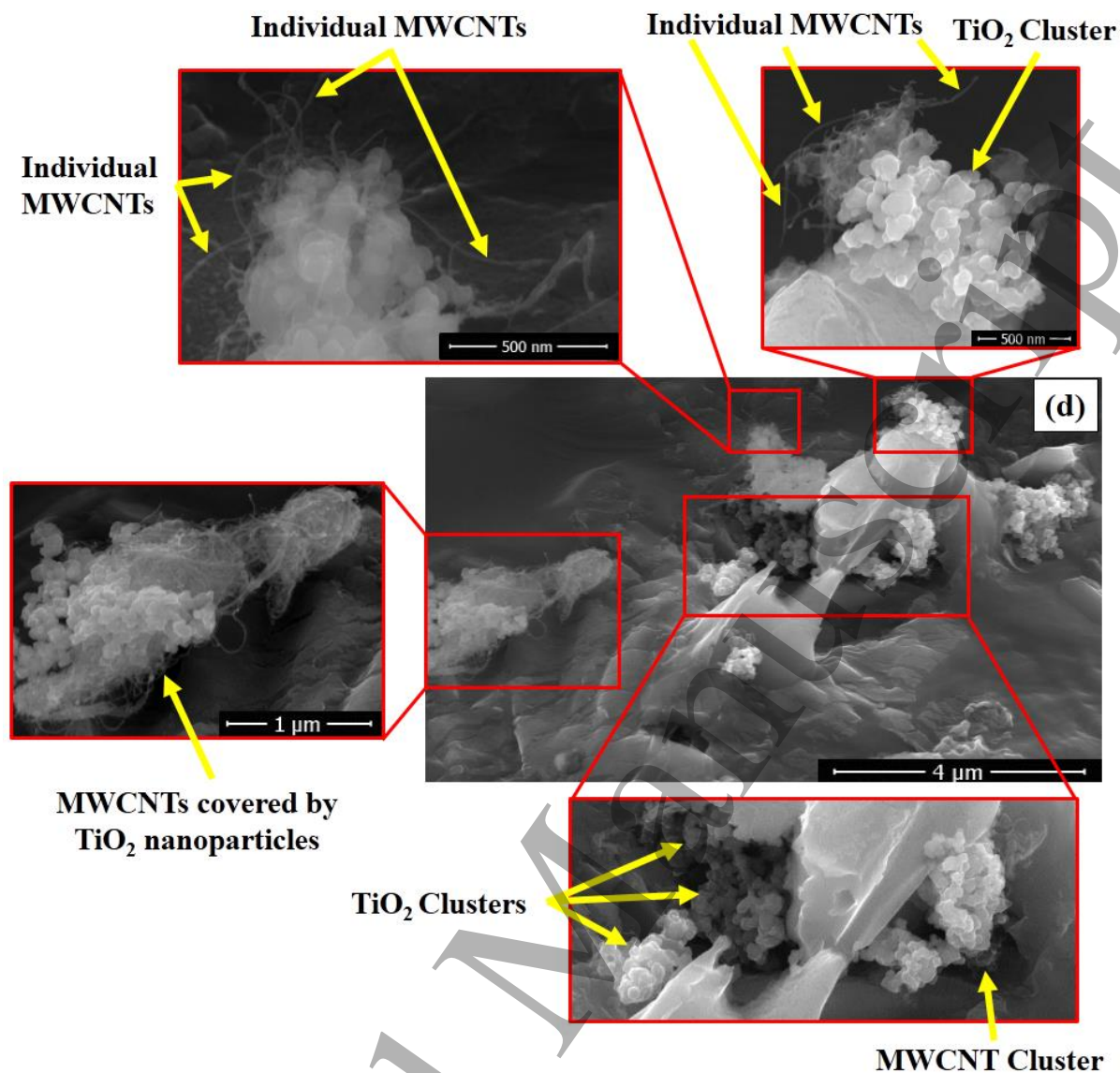
Fig. 27. High-magnification SEM and FE-SEM images of the tensile tested specimens of (a) NC1, (b) HNC1, (c) HNC2 and (d) HNC3.

FE-SEM image of the HNC6 (**Fig. 28b**), confirms the presence of broken MWCNTs and individual untangled MWCNT ropes (pulled-out nanotubes) due to the uniform dispersion of nanoparticles within the matrix, which agrees well with the TEM observations (**Fig. 18**). These untangled and individual MWCNT ropes are needed for effective load transfer (strong interface) among the matrix and reinforcement and may also prevent early fracture during the application of tensile load [48]. Moreover, EDS analysis shows clear evidence of nanoparticle mixture in the fracture surfaces of HNC6 (**Fig. 28a**). The above findings reveal that there is a strong interfacial bonding among the MWCNTs and Al6061 matrix in the HNC6, where the

embedded MWCNTs are very difficult to pull out from the Al6061 matrix. This pull-out difficulty of MWCNTs from the Al6061 matrix is very beneficial for the effective transfer of the load from Al6061 to the MWCNTs and enhancement on the mechanical properties of the hybrid nanocomposite.
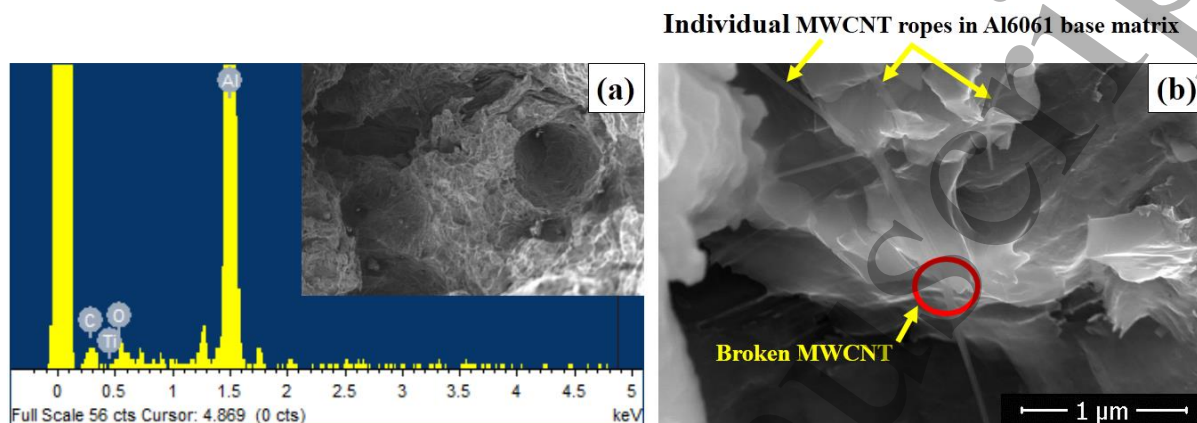

Fig. 28. (a) EDX with fracture area of HNC6 (inside) and (b) FESEM image of HNC6 fracture surface showing individual MWCNT ropes and broken MWCNT.

Outcomes obtained from the microstructure and mechanical characterization demonstrate the importance of analyzing the different reinforcements pre-processing routes and their effect on mechanical and physical properties of resulting nanocomposites. From these outcomes, it is clearly observed that the MWCNTs shortening by using prolong ball-milling time is an effective approach to attain uniform dispersion of nanotubes as well as TiO_2 nanoparticles in ultrasonic-assisted casting technique, and causing a significant strengthening of the hybrid nanocomposite. The average particle size of the 6 h ball-milled TiO_2/MWCNT nanoparticles mixture was refined to about 3.88 µm. Consequently, the size of the nanoparticles agglomerates in hybrid nanocomposites significantly reduced (**Figs. 21h-i**) due to the combined effect of reinforcement pre-processing and ultrasonic treatment, which strongly contributes to the improvement of the tensile strength of the resulting nanocomposites. Therefore, difficulties associated with a uniform dispersion of nanomaterials and nanoparticles in the casting technique is resolved up to some extent. Furthermore, ball-milling and sonication time of more than 20 min and 6 h may be beneficial for further improvement in mechanical properties of

resulting nanocomposites, but destruction in nanotubes morphology is one of the significant constraints, which was earlier experienced by various researchers [17,34].

Based on the obtained results, it can be concluded that to attain uniform dispersion of nanoparticles in the molten melt, ultrasonic-assisted stirring alone was not enough, hence pre-processing of reinforcements is strongly recommended especially in case of nanomaterials (CNTs) and nanoparticles.

4. Conclusions

In the present work, an effort has been made to diminish the agglomeration of nano-reinforcements in Al6061-TiO$_2$-MWCNT hybrid nanocomposites by using a combined approach of reinforcement pre-processing and ultrasonic-assisted casting. The effect of different dispersion routes on the microstructure and strengthening of ultrasonic-assisted stir/squeeze cast hybrid nanocomposites were investigated. The present investigation led to the following conclusions:

➤ Morphological characterization of MWCNTs revealed that the sonication time of 20 min is sufficient to obtain the dispersion uniformity, and further increment in the sonication period leads to agglomeration and destruction in their tubular morphology. However, microstructure investigation of MWCNTs dispersed through prolonged ball milling (up to 6 h) exhibited MWCNTs shortening (change in aspect ratio) due to the shearing effects of the balls.

➤ It is observed that the trivial loading of pre-processed TiO$_2$ (1 wt%)/MWCNT (1.5 wt%) nanoparticles in the Al6061 matrix significantly increases the UTS, YS and microhardness of the hybrid nanocomposites. The combined approach of nano-reinforcement pre-processing and ultrasonic-assisted casting was found to be an effective technique for preparing Al6061-TiO$_2$-MWCNT hybrid nanocomposites.

➤ It is observed from present work that the 6 h ball-milling (R4) is a promising approach to achieve the uniform mixing and dispersion of TiO_2/MWCNT nanoparticles and causing a significant improvement in the mechanical properties of the resulting hybrid nanocomposites. It is also observed that sonication alone or ball milling (up to 1 h) is not sufficient to achieve the desired dispersion uniformity of the nano-reinforcements.

➤ The ultrasonic-assisted squeeze cast HNC7 showed higher UTS, YS and microhardness over the stir cast HNC6 due to the secondary material processing technique, uniform dispersion of nano-reinforcements and ultra-level grain refinement.

➤ From the outcomes of the microstructure and mechanical properties investigations, it is evident that the substantial enhancement in the UTS, YS and microhardness of the hybrid nanocomposites is associated with the nanoparticle strengthening effects, grain size refinement and uniform dispersion of TiO_2/MWCNT nanoparticles.

➤ The FE-SEM investigation on hybrid nanocomposites fractured surface confirms the presence of TiO_2 and MWCNT nanoparticles without any sign of destruction in their morphology.

Finally, it can be concluded that the proposed new reinforcement dispersion/pre-processing route diminishes the agglomeration effect of TiO_2/MWCNT nanoparticles as well as strengthen the resulting hybrid nanocomposite remarkably. Hence, to utilize the utmost properties of reinforcing materials, pre-processing of reinforcement is strongly recommended for the fabrication of composites reinforced with nanoparticles (especially for nanomaterials) in the casting approach. Moreover, the proposed AMMHNCs with improved mechanical characteristics make it a suitable candidate for employment in the aerospace and automotive sectors, where compromise in quality is undesirable.

1
2
3
4
5
6
7
8
9
10
11
12
13
14
15
16
17
18
19
20
21
22
23
24
25
26
27
28
29
30
31
32
33
34
35
36
37
38
39
40
41
42
43
44
45
46
47
48
49
50
51
52
53
54
55
56
57
58
59
60

Acknowledgments

References

[1]   Iijima S 1991 Helical microtubules of graphitic carbon *Nature* **354** 56–8

[2]   Treacy M M J, Ebbesen T W and Gibson J M 1996 Exceptionally high Young's modulus observed for individual carbon nanotubes *Nature* **381** 678–80

[3]   Demczyk B G, Wang Y M, Cumings J, Hetman M, Han W and Zettl A 2002 Direct mechanical measurement of the tensile strength and elastic modulus of multiwalled carbon nanotubes **334** 173–8

[4]   Radhamani A V., Lau H C and Ramakrishna S 2018 CNT-reinforced metal and steel nanocomposites: A comprehensive assessment of progress and future directions *Compos. Part A Appl. Sci. Manuf.* **114** 170–87

[5]   Azarniya A, Azarniya A, Sovizi S, Hosseini H R M, Varol T, Kawasaki A and Ramakrishna S 2017 Physicomechanical properties of spark plasma sintered carbon nanotube-reinforced metal matrix nanocomposites *Prog. Mater. Sci.* **90** 276–324

[6]   Silvestre N 2013 State-of-the-art Review on Carbon Nanotube Reinforced Metal Matrix Composites *Int. J. Compos. Mater.* **3** 28–44

[7]   Huang Y, Ouyang Q, Zhang D, Zhu J, Li R and Yu H 2014 Carbon materials reinforced aluminum composites: A review *Acta Metall. Sin. (English Lett.* **27** 775–86

[8]   Koli D K, Agnihotri G and Purohit R 2015 Advanced Aluminium Matrix Composites: The Critical Need of Automotive and Aerospace Engineering Fields *Mater. Today Proc.* **2** 3032–41

[9]   Kumar V M and Venkatesh C V 2019 A comprehensive review on material selection, processing, characterization and applications of aluminium metal matrix composites

Mater. Res. Express **6**

[10] Macke A and Schultz Pradeep Rohatgi B 2012 Metal Matrix Composites Offer the Automotive Industry an Opportunity to Reduce Vehicle Weight, Improve Performance Property Materials Application metal-matrix composite (mmc) materials being developed at university of wisconsin-milwaukee for use in automo 19–23

[11] Liu Q, Ke L, Liu F, Huang C and Xing L 2013 Microstructure and mechanical property of multi-walled carbon nanotubes reinforced aluminum matrix composites fabricated by friction stir processing *Mater. Des.* **45** 343–8

[12] Du Z, Tan M J, Guo J F, Bi G and Wei J 2016 Fabrication of a new Al-Al2O3-CNTs composite using friction stir processing (FSP) *Mater. Sci. Eng. A* **667** 125–31

[13] Liu Z Y, Zhao K, Xiao B L, Wang W G and Ma Z Y 2016 Fabrication of CNT/Al composites with low damage to CNTs by a novel solution-assisted wet mixing combined with powder metallurgy processing *Mater. Des.* **97** 424–30

[14] Van Trinh P, Van Luan N, Minh P N and Phuong D D 2017 Effect of Sintering Temperature on Properties of CNT/Al Composite Prepared by Capsule-Free Hot Isostatic Pressing Technique *Trans. Indian Inst. Met.* **70** 947–55

[15] Samuel Ratna Kumar P S, Robinson Smart D S and John Alexis S 2017 Corrosion behaviour of Aluminium Metal Matrix reinforced with Multi-wall Carbon Nanotube *J. Asian Ceram. Soc.* **5** 71–5

[16] Uozumi H, Kobayashi K, Nakanishi K, Matsunaga T, Shinozaki K, Sakamoto H, Tsukada T, Masuda C and Yoshida M 2008 Fabrication process of carbon nanotube/light metal matrix composites by squeeze casting *Mater. Sci. Eng. A* **495** 282–7

[17] Simões S, Viana F, Reis M A L and Vieira M F 2015 Influence of dispersion/mixture time on mechanical properties of Al–CNTs nanocomposites *Compos. Struct.* **126** 114–22

[18] Alizadeh A and Abdollahi A 2015 Creep Behavior and Wear Resistance of Al 5083 Based Hybrid Composites Reinforced with Carbon Nanotubes (CNTs) and Boron Carbide (B4C) *J. Alloys Compd.* **650** 783–93

[19] Yazdani B, Xu F, Ahmad I, Hou X, Xia Y and Zhu Y 2015 Tribological performance of Graphene/Carbon nanotube hybrid reinforced Al2O3 composites *Sci. Rep.* **5** 1–11

[20] So K P, Jeong J C, Park J G, Park H K, Choi Y H, Noh D H, Keum D H, Jeong H Y, Biswas C, Hong C H and Lee Y H 2013 SiC formation on carbon nanotube surface for improving wettability with aluminum *Compos. Sci. Technol.* **74** 6–13

[21] Abraham S J, Dinaharan I, Selvam J D R and Akinlabi E T 2018 Microstructural Characterization and Tensile Behavior of Rutile (TiO2)- Reinforced AA6063 Aluminum Matrix Composites Prepared by Friction Stir Processing *Acta Metall. Sin. (English Lett.* **32** 52–62

[22] Agarwal P, Kishore A, Kumar V, Soni S K and Thomas B 2019 Fabrication and machinability analysis of squeeze cast Al 7075/ h-BN/graphene hybrid nanocomposite *Eng. Res. Express* **1** 015004

[23] Abdizadeh H, Ebrahimifard R and Baghchesara M A 2014 Investigation of microstructure and mechanical properties of nano MgO reinforced Al composites manufactured by stir casting and powder metallurgy methods: A comparative study *Compos. Part B Eng.* **56** 217–21

[24] Reddy A P, Krishna P V and Rao R N 2019 Strengthening and Mechanical Properties of SiC and Graphite Reinforced Al6061 Hybrid Nanocomposites Processed Through Ultrasonically Assisted Casting Technique *Trans. Indian Inst. Met.* **72** 2533–2546

[25] Srivastava N and Chaudhari G P 2016 Strengthening in Al alloy nano composites fabricated by ultrasound assisted solidification technique *Mater. Sci. Eng. A* **651** 241–7

[26] Manivannan I, Ranganathan S, Gopalakannan S and Suresh S 2018 Mechanical Properties and Tribological Behavior of Al6061–SiC– Gr Self-Lubricating Hybrid Nanocomposites *Trans. Indian Inst. Met.* **71** 1897–911

[27] Kannan C and Ramanujam R 2018 Effectiveness evaluation of molten salt processing and ultrasonic cavitation techniques during the production of aluminium based hybrid nanocomposites - An experimental investigation *J. Alloys Compd.* **751** 183–93

[28] Harichandran R and Selvakumar N 2018 Microstructure and mechanical characterization of (B 4 C + h-BN)/Al hybrid nanocomposites processed by ultrasound assisted casting *Int. J. Mech. Sci.* **144** 814–26

[29] Dorri Moghadam A, Omrani E, Lopez H, Zhou L, Sohn Y and Rohatgi P K 2017 Strengthening in hybrid alumina-titanium diboride aluminum matrix composites

synthesized by ultrasonic assisted reactive mechanical mixing Afsaneh *Mater. Sci. Eng. A* **702** 312–21

[30] Shayan M, Eghbali B and Niroumand B 2019 Synthesis of AA2024-(SiO2np+TiO2np) hybrid nanocomposite via stir casting process Mehrdad *Mater. Sci. Eng. A* **756** 484–91

[31] Xu R, Tan Z, Xiong D, Fan G, Guo Q, Zhang J, Su Y, Li Z and Zhang D 2017 Balanced strength and ductility in CNT/Al composites achieved by flake powder metallurgy via shift-speed ball milling *Compos. Part A Appl. Sci. Manuf.* **96** 57–66

[32] Trinh P Van, Luan N Van, Dinh D, Ngoc P, Weibel A, Mesguich D and Laurent C 2018 Microstructure, microhardness and thermal expansion of CNT/Al composites prepared by flake powder metallurgy *Compos. Part A* **105** 126–37

[33] Phuong D D, Trinh P Van, An N Van, Luan N Van, Minh P N, Khisamov R K, Nazarov K S, Zubairov L R, Mulyukov R R and Nazarov A A 2014 Effects of carbon nanotube content and annealing temperature on the hardness of CNT reinforced aluminum nanocomposites processed by the high pressure torsion technique *J. Alloys Compd.* **613** 68–73

[34] Liu Z Y, Xu S J, Xiao B L, Xue P, Wang W G and Ma Z Y 2012 Effect of ball-milling time on mechanical properties of carbon nanotubes reinforced aluminum matrix composites *Compos. Part A Appl. Sci. Manuf.* **43** 2161–8

[35] Sharma N, Syed A N, Ray B C, Yadav S and Biswas K 2019 Alumina–MWCNT composites: microstructural characterization and mechanical properties *J. Asian Ceram. Soc.* **7** 1–19

[36] Dai S, Wu Y, Sakai T, Du Z, Sakai H and Abe M 2010 Preparation of Highly Crystalline TiO2 Nanostructures by Acid-assisted Hydrothermal Treatment of Hexagonal-structured Nanocrystalline Titania/Cetyltrimethyammonium Bromide Nanoskeleton *Nanoscale Res. Lett.* **5** 1829–35

[37] Orge C A, Soares O S G P, Faria J L and Pereira M F R 2017 Synthesis of TiO2-Carbon Nanotubes through ball-milling method for mineralization of oxamic acid (OMA) by photocatalytic ozonation *J. Environ. Chem. Eng.* **5** 5599–607

[38] Kannan C, Ramanujam R and Balan A S S 2018 Machinability studies on Al 7075/BN/Al2O3 squeeze cast hybrid nanocomposite under different machining

environments *Mater. Manuf. Process.* **33** 587–95

[39] Kannan C and Ramanujam R 2017 Comparative study on the mechanical and microstructural characterisation of AA 7075 nano and hybrid nanocomposites produced by stir and squeeze casting *J. Adv. Res.* **8** 309–19

[40] Rajmohan T, Palanikumar K and Arumugam S 2014 Synthesis and characterization of sintered hybrid aluminium matrix composites reinforced with nanocopper oxide particles and microsilicon carbide particles *Compos. Part B Eng.* **59** 43–9

[41] Singh J and Chauhan A 2016 Characterization of hybrid aluminum matrix composites for advanced applications – A review *J. Mater. Res. Technol.* **5** 159–69

[42] Prasad Reddy A, Vamsi Krishna P and Rao R N 2019 Tribological Behaviour of Al6061–2SiC-xGr Hybrid Metal Matrix Nanocomposites Fabricated through Ultrasonically Assisted Stir Casting Technique *Silicon* 1–19

[43] S.V.Alagarsamy and M.Ravichandran 2019 Synthesis, microstructure and properties of TiO2 reinforced AA7075 matrix composites via stir casting route *Mater. Res. Express* **6** 086519

[44] Evgin T, Turgut A, Šlouf M, Špitalsky Z, Micusik M, Sarıkanat M, Nogellova Z, Novak I and Omastová M 2019 Morphological, electrical, mechanical and thermal properties of high-density polyethylene/multiwall carbon nanotube nanocomposites: effect of aspect ratio *Mater. Res. Express* **6** 095079

[45] Kumar K A, Natarajan S, Duraiselvam M and Ramachandra S 2019 Synthesis, characterization and mechanical behavior of Al 3003 - TiO2 surface composites through friction stir processing *Mater. Manuf. Process.* **34** 183–91

[46] Zhang Z and Chen D L 2008 Contribution of Orowan strengthening effect in particulate-reinforced metal matrix nanocomposites *Mater. Sci. Eng. A* **483**–**484** 148–52

[47] Pazhouhanfar Y and Eghbali B 2018 Microstructural characterization and mechanical properties of TiB2 reinforced Al6061 matrix composites produced using stir casting process *Mater. Sci. Eng. A* **710** 172–80

[48] He C N, Feng C, Lin J C, Liu E Z, Shi C S, Li J J and Zhao N Q 2016 Fabrication of Carbon Nanotube-Reinforced 6061Al Alloy Matrix Composites by an In Situ Synthesis Method Combined with Hot Extrusion Technique *Acta Metall. Sin. (English Lett.* **29**

188–98